Journal of Neuroscience Research 86:1994–2002 (2008)

MBNL1 Associates with YB-1 in Cytoplasmic Stress Granules

Hayato Onishi,[1] Yoshihiro Kino,[1,2] Tomoko Morita,[1] Eugene Futai,[1] Noboru Sasagawa,[1] and Shoichi Ishiura[1]*

[1]Department of Life Sciences, Graduate School of Arts and Sciences, University of Tokyo, Tokyo, Japan
[2]Laboratory for Structural Neuropathology, Brain Science Institute, RIKEN, Tokyo, Japan

The muscleblind-like (MBNL) protein family is thought to be involved in the molecular mechanism of myotonic dystrophy (DM). Although it has been shown to have splicing activity, a broader function in cellular RNA metabolism has been implicated. In this study, we attempted to find the binding proteins of MBNL1 in order to elucidate its physiological function. First, we performed a GST pull-down assay using GST-MBNL1-6xHis as bait. Several proteins were identified, including YB-1, a multifunctional DNA/RNA-binding protein, and DDX1, a DEAD box RNA helicase. MBNL1 formed an RNP complex with YB-1 and DDX1 in binding assays. YB-1 also showed a weak but significant effect on α-actinin splice site selection. Interestingly, in response to stress, MBNL1 moved to cytoplasmic stress granules, where it colocalized with YB-1, which was previously reported to be a component of stress granules. We found that DDX1 also colocalized with MBNL1 at stress granules. These results provide new insight into the dynamics of MBNL1 in response to stress, and they suggest a role for MBNL1 in mRNA metabolism in the cytoplasm.

Key words: myotonic dystrophy; MBNL1; YB-1; stress granules; splicing

Myotonic dystrophy (dystrophia myotonica; DM) is one of the most common human muscular dystrophies, occurring at a frequency of 1 in 8,000 (Harper, 2001). The clinical features of DM include myotonia, cataracts, insulin resistance, and cognitive dysfunction (Meola et al., 2003). DM is an autosomally inherited disorder that is classified into two types, DM1 and DM2, based on the expansion of tri (CTG)- and tetra (CCTG)-nucleotide repeats in the 3′-UTR of *DMPK* (Brook et al., 1992; Mahadevan et al., 1992; Fu et al., 1993) and intron 1 of *ZNF9* (Liquori et al., 2001), respectively. DM1 and DM2 have similar phenotypes even though they are caused by unrelated mutations (Day et al., 2003). Various hypotheses have been proposed to explain how untranslated mutations can lead to a dominant pathogenic phenotype; however, several lines of evidence support a "gain-of-function" model for expanded RNA repeats. No DMPK mutation except for the repeat expansion has ever been reported, indicating that loss of function of DMPK is not the major cause of DM1. Although mice deficient in DMPK show mild myopathy and abnormalities in cardiac conductance, they do not reproduce other symptoms of DM1 (Jansen et al., 1996; Reddy et al., 1996; Berul et al., 1999). On the other hand, mice expressing expanded CUG repeats inserted in the 3′-UTR of the muscle-specific actin gene developed myotonia and DM-like myopathy (Mankodi et al., 2000). There are several reports that CUG or CCUG repeat RNAs form nuclear foci in cells or tissues of DM1 or DM2 patients and mice expressing expanded CUG repeats by using fluorescent in situ hybridization (FISH; Taneja et al., 1995; Davis et al., 1997; Amack et al., 1999; Mankodi et al., 2000, 2001; Liquori et al., 2001). This evidence suggests that the expressions of expanded CUG or CCUG repeats are likely to be central features and sufficient for causing these symptoms.

The RNA repeat foci seem to sequester several RNA binding proteins, such as those of the well-known MBNL family (Fardaei et al., 2001, 2002; Mankodi et al., 2001). MBNL1, which has four Cys_3His zinc-finger domains, is a human homologue of *Drosophila* muscleblind (Begemann et al., 1997), which has been reported to play some role in the differentiation of eye and muscle (Begemann et al., 1997; Artero et al., 1998). MBNL1 was first isolated as a CUG repeat binding protein in relation to DM (Miller et al., 2000). Previously, the binding specificity of MBNL1 was characterized, and target RNA sequence was determined (Kino et al., 2004). The MBNLs have been established as regulators of alternative splicing (Ho et al., 2004). Recently, it was

Supplementary Material for this article is available online at http://www.mrw.interscience.wiley.com/suppmat/0360-4012/suppmat/ (www.interscience.wiley.com).

Contract grant sponsor: Ministry of Health, Labor and Welfare, Japan; Contract grant sponsor: HFSP.

*Correspondence to: Shoichi Ishiura, Department of Life Sciences, Graduate School of Arts and Sciences, University of Tokyo, Tokyo, Japan. E-mail: cishiura@mail.ecc.u-tokyo.ac.jp

Received 2 October 2007; Revised 30 November 2007; Accepted 17 December 2007

Published online 11 March 2008 in Wiley InterScience (www.interscience.wiley.com). DOI: 10.1002/jnr.21655

suggested that *Muscleblind* has a role in translational control through a modulation of RNA stability in the cytoplasm (Houseley et al., 2005). In addition, it was shown that localized expression of the integrin α3 is regulated at the level of RNA localization by MBNL2 (MLP1), a human paralogue of MBNL1 (Adereth et al., 2005). These findings imply that MBNL1 might also have a similar role in mRNA metabolism in the cytoplasm. The physiological functions of MBNL1 are largely unknown except that it has splicing activity and its function is down-regulated in DM. Although therapeutic strategies that restore MBNL1 function to normal would likely benefit those with DM, a broader understanding of MBNL1 function is important for elucidating DM pathogenesis.

MATERIALS AND METHODS

Plasmid Construction

The open reading frames for *YB-1*, *DDX1*, *TIA-1*, and *DCP2* were amplified by PCR from a human skeletal muscle cDNA library (Clontech, Logan, UT) and cloned into pcDNA3.1-V5 (Invitrogen, Carlsbad, CA), pECFP-C1 (Clontech), or pcDNA3-HA (Invitrogen) using conventional molecular biological techniques. $MBNL1_{40}$ was cloned into pEGFP-N1 (Clontech) or pSecDk. The pSecDk vector was generated by deleting the IgG sequence from pSecTagA (Invitrogen). The EF1-EF2 region of α-actinin was amplified by PCR from rat genome DNA and cloned into the BglII-SalI site of pEGFP-C1 (Clontech). The nucleotide sequences of the DNA inserts were confirmed by sequencing.

Antibodies

Anti-MBNL1 rabbit polyclonal antibodies were raised using bacterially expressed $MBNL1_{40}$-6xHis as the antigen. The serum was purified with $MBNL1_{40}$-coupled Affigel 10 (Bio-Rad, Hercules, CA) and cleared by GST-6xHis-bound glutathione Separose (Amersham, Arlington Heights, IL). Goat anti-TIA-1 was purchased from Santa Cruz Biotechnology (Santa Cruz, CA). Rat anti-HA 3F10 was purchased from Roche (Indianapolis, IN). Mouse anti-V5 and anti-myc antibodies were purchased from Invitrogen. Alexa Fluor 568-labeled goat anti-mouse IgG, Alexa Fluor 488-labeled donkey anti-rabbit IgG, Alexa Fluor 546-labeled donkey anti-goat IgG, and Alexa Fluor 488-labeled donkey anti-rat IgG were purchased from Molecular Probes (Eugene, OR).

Protein Purification

Recombinant GST-$MBNL1_{40}$-6xHis was expressed in bacteria and purified as described elsewhrere (Kino et al., 2004). Briefly, pET-GX containing $MBNL1_{40}$ was transformed into BL21 (DE3) cells and cultured overnight in LB medium. The culture was then diluted and shaken at 37°C for 1.5 hr, or until the OD_{600} reached 0.3–0.4, and then 0.2 mM IPTG was added. During induction, the culture was shaken at 25°C for 4 hr. The bacterial cells were then collected and lysed twice in a French pressure cell press (Ohtake Works, Co.) before being centrifuged at 5,000*g* for 20 min. The supernatant was subjected to affinity purification using glutathione Sepharose 4B (Amersham Biosciences). The beads were washed with ATP $MgSO_4$ buffer to exclude DnaK, and GST-$MBNL1_{40}$-6xHis was eluted with 50 mM Tris-HCl, pH 8.8, and 10 mM glutathione (reduced type). The eluate was then mixed with NaCl and imidazole before the addition of Talon Metal Affinity Resin (Clontech) according to the manufacturer's protocol. Finally, the purified proteins were dialyzed against a stock buffer (50 mM Tris-HCl, pH 8.0, 100 mM NaCl, and 2 mM 2-mercaptoethanol). The quantity and purity of the samples were checked by SDS-PAGE with Coomassie brilliant blue (CBB) staining. The identity of GST-$MBNL1_{40}$-6xHis was confirmed by peptide mass fingerprinting with mass spectrometry (AXIMA-CFR, Shimadzu) following digestion with trypsin.

GST Pull-Down Assay

Mouse muscle and heart (2 g each) were homogenized in lysis buffer (50 mM Tris-HCl, pH 8.0, 100 mM NaCl, 2 mM 2-mercaptoethanol, 0.5% NP-40, 0.5% Triton X-100, and 1/1,000 vol protease inhibitors) using a Hitachi homogenizer and centrifuged at 15,000*g* for 20 min. Next, the supernatant was precleared with 500 μl of glutathione Sepharose for 2 hr and with GST-6xHis-bound glutathione Sepharose for 2 hr at 4°C. Finally, the supernatant was mixed with 20 μg of GST-$MBNL1_{40}$-6xHis and rotated overnight at 4°C. The beads were washed five times with lysis buffer, and the complex was eluted by cleavage with 3 U thrombin for 1 hr at 20°C, then subjected to SDS-PAGE.

In-Gel Trypsin Digestion and Analysis by Matrix-Assisted Laser Desorption/Ionization Tandem Time-of-Flight (MALDI-TOF/TOF) Mass Spectrometry

Pull-down assays were performed as described above. The bound proteins were separated by 12.5% SDS-PAGE and stained with Silver Quest (Invitrogen). The bands were excised from the gel and destained, dehydrated with acetonitrile for 10 min, and dried completely under a vacuum pump for 10 min. Each band was placed in 20 μl of 5 mM NH_4HCO_3 containing 1 pmol sequencing-grade trypsin (Promega, Madison, WI) at 37°C overnight. Aliquots of the trypsinized samples were analyzed by nanoliquid chromatography and automatically spotted with alfa-cyano-4-hydroxyl-cinnamic acid solution on a stainless-steel target and air dried. MALDI-TOF/TOF analysis was conducted with a Proteomics analyzer 4700 (Applied Biosystem, Foster City, CA). The proteins were identified by database searches on the web with Mascot (Matrix Science, Ltd., London, United Kingdom).

Western Blotting

The samples were subjected to 10% SDS-PAGE and transferred to PVDF membranes (Immobilon-P; Millipore, Bedford, MA). The membranes were then blocked with 5% skim milk in TPBS (0.05% Tween 20 in PBS) for 1 hr at room temperature and incubated with primary antibodies in TPBS. After washing, the membranes were incubated for 1 hr with horseradish peroxidase (HRP)-conjugated secondary antibodies. The immunoreactive bands were visualized with the LAS-3000 imaging system (Fujifilm, Tokyo, Japan).

Immunoprecipitation

COS-7 cells were transfected with myc-tagged constructs of MBNL1 and V5-tagged constructs of YB-1 or DDX1 using FuGENE6 (Roche, Basel, Switzerland). Cells from two 10-cm plates were homogenized in 500 μl lysis buffer [50 mM Tris-HCl, pH 8.0, 150 mM NaCl, 5 mM dithiothreitol (DTT), 1 mM EDTA, 1% (w/v) Triton X-100, and protease inhibitor cocktail]. The lysates were then centrifuged at 100,000*g* for 15 min at 4°C. The supernatant was precleared with protein G Sepharose 4 fast flow beads (Amersham Biosciences, Piscataway, NJ) for 1 hr and then incubated with anti-V5 antibodies fixed on beads. After the beads were washed five times with lysis buffer, the precipitates were analyzed by SDS-PAGE and immunoblotted with either anti-myc or anti-V5 antibodies.

Immunocytochemistry and Image Analysis

HeLa and COS-7 cells were fixed with PBS containing 4% (w/v) paraformaldehyde for 15 min and permeabilized with 0.1% (w/v) Triton X-100 in PBS for 15 min. After the buffer was exchanged for 3% (w/v) BSA in PBS, the cells were incubated with the first antibody in 3% BSA in PBS for 1 hr, washed with PBS, and then incubated with the second antibody in 3% BSA in PBS for 1 hr. After washing with PBS, the samples were embedded in Mowiol (Calbiochem, La Jolla, CA). Cell images were acquired on a Zeiss LSM510 Meta laser scanning confocal microscope (Carl Zeiss, Jena, Germany) or IX70 microscope (Olympus, Tokyo, Japan).

Polysome Analysis

HeLa (10-cm dish) cells were exposed to 50 μg/ml cycloheximide at 37°C for 10 min, washed twice with cold PBS, and resuspended in 300 μl TKM buffer (10 mM Tris-HCl, pH 7.5, 100 mM KCl, 5 mM $MgCl_2$, and 50 μg/ml cycloheximide). The cells were then homogenized by passing them through a 27-gauge needle 10 times. Both the PBS and the TKM contained 50 μg/ml cycloheximide. The homogenate was centrifuged at 2,000*g* for 10 min at 4°C, and the supernatant was then loaded onto a gradient of 15–40% (w/v) sucrose in TKM and sedimented for 60 min at 4°C at 40,000 rpm (18 kG) in a swinging bucket rotor. The gradient was collected in 15 fractions, with concomitant measurement of the absorbance at 254 nm. The proteins were precipitated with trichloroacetic acid and subjected to SDS-PAGE and Western blot analysis, as described above.

Splicing Assays

For the in vivo splicing assays, HEK293 cells were plated in 3.5-cm or 6-cm dishes and cultured for 24 hr in DMEM plus 10% FBS before plasmid transfection. Cells were grown to 60–80% confluence and then transiently cotransfected using FuGENE 6 (Roche) according to the manufacturer's instructions with 300 ng splicing reporter and 4 μg YB-1-V5, MBNL1-myc, or DDX1-V5. The cells were collected after 48 hr, total RNA was extracted using an RNeasy Kit (Qiagen, Valencia, CA), and the samples were analyzed by RT-PCR. Reverse-transcription was done by using PrimeScript Reverse Transcriptase (TaKaRa). Spliced products were amplified using EGFP primer (Fw: CATGGTCCTGCTGGAGTTCGTG, Rv: GTTTCAGGTTCAGGGGGAGGTGTG) and separated by 6% polyacrylamide gel.

RESULTS

Pull-Down Screening of MBNL1

MBNL1 has nine splicing isoforms (Kino et al., 2004; Pascual et al., 2006). The ratio of each isoform is likely to change during development and differentiation of muscle (Kanadia et al., 2006). Recently, it was shown that MBNL2 (MLP1) is involved in the local translation of the integrin α3 by transporting the transcript to specific points in the cytoplasm (Adereth et al., 2005). Therefore, we focused on both the nuclear and the cytosolic compartment of MBNL1, and we selected $MBNL1_{40}$, which localizes to both compartments, for use as bait in a GST pull-down assay. Double-tagged GST-MBNL1-6xHis was purified in a two-step procedure. Purified GST-MBNL1-6xHis was bound to glutathione beads and mixed with a mouse muscle or heart lysate. After incubation overnight, the beads were washed extensively, and the proteins were eluted by thrombin cleavage. After elution, the complexes in the experimental and control samples were compared by SDS-PAGE (Fig. 1). About 20 bands were detected in the sample containing muscle lysate as prey. Each band was excised from the gel and digested with trypsin. The trypsinized peptides were then subjected to MADLI-TOF/TOF analysis, and each protein was identified in MASCOT software (Suppl. Table I). Seven proteins among 20 bands were identified, and these were YB-1, DDX1, phenylalaninyl-tRNA synthetase α and β subunits, amylo-1,6-glucosidase, and several small and large ribosomal subunits. YB-1 is a multifunctional RNA/DNA binding protein and has a role in transcriptional and posttranscriptional RNA metabolism, including splicing (Stickeler et al., 2001; Rapp et al., 2002; Kohno et al., 2003; Raffetseder et al., 2003; Allemand et al., 2007). DDX1 is part of the DEAD box RNA helicase family (Cordin et al., 2006). From all of the proteins identified, we focused our attention on the two proteins known to be involved in mRNA metabolism.

Interactions Between MBNL1 and YB1 or DDX1

To confirm the interaction between MBNL1 and YB-1 or DDX1, we performed a pull-down assay. Forty-eight hours after transfection with YB-1-V5 or DDX1-V5, each COS-7 lysate was mixed with GST-$MBNL1_{40}$-6xHis bound to glutathione Sepharose. After 4 hr, the beads were washed thoroughly and boiled in SDS sample buffer. The binding of these proteins was confirmed (Fig. 2A). As negative controls, RNA binding proteins HuR and calreticulin were shown not to bind MBNL1 (data not shown). Next, immunoprecipitation (IP) assays were performed against MBNL1-myc and YB-1-V5 expressed in COS-7 (Fig. 2B). MBNL1-myc

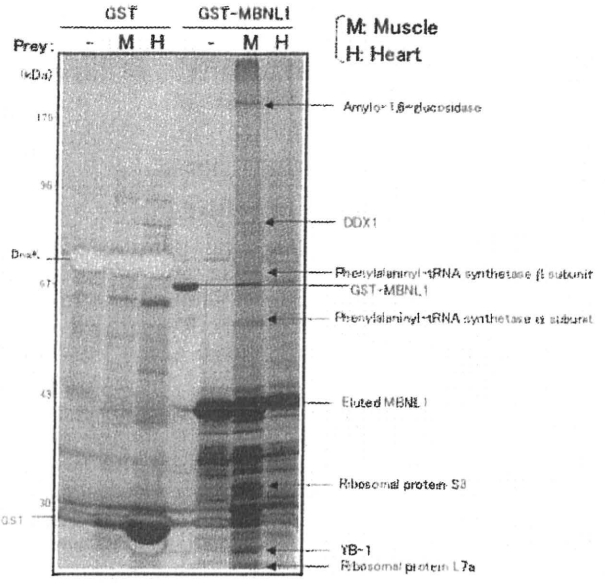

Fig. 1. GST pull-down assay with $MBNL1_{40}$. Identification of $MBNL1_{40}$-interacting proteins by pull-down assay and mass spectrometry. GST-$MBNL1_{40}$-6xHis (20 μg) or GST-6xHis (20 μg) was incubated for 16 hr with 2 g mouse muscle (M) or heart (H) lysate. The MBNL1 complex was eluted by thrombin cleavage. Twenty bands that were reproducibly observed in the GST-$MBNL1_{40}$-6xHis pull-down with muscle were subjected to MALDI-TOF/TOF analysis and identified as indicated. Accession Nos. are as follows: amylo-1,6-glucosidase, XM_131166.8; DEAD (Asp-Glu-Ala-Asp) Box polypeptide 1, NM_134040.1; phenylalanyl-tRNA synthetase α subunit, NM_011811.3; phenylalanyl-tRNA synthetase β subunit, NM_025648.2; ribosomal protein S3, NM_012052.2; Y-box transcription factor, NM_011732; and ribosomal protein L7a, NM_013721.3.

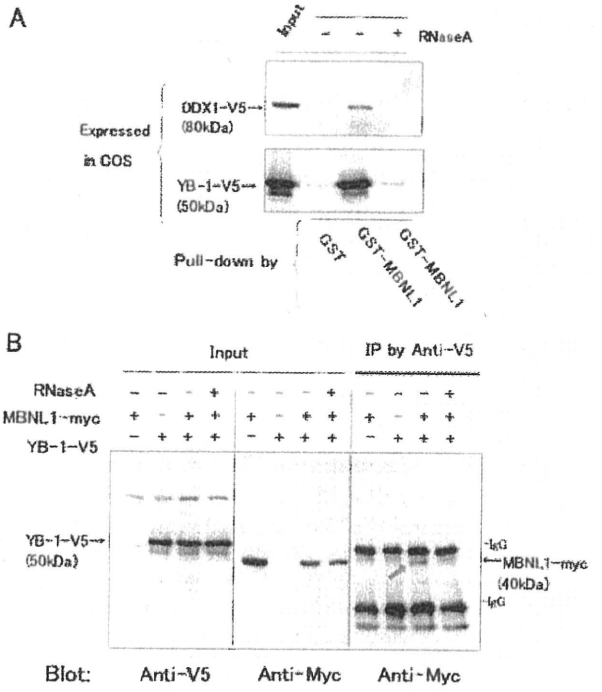

Fig. 2. Interactions of MBNL1 with YB1 or DDX1 **A:** Pull-down assays were performed with GST-$MBNL1_{40}$-6xHis as bait. In the upper panel, transiently expressed DDX1- or YB-1-V5 was pulled-down by GST-$MBNL1_{40}$-6xHis. Binding was diminished by the addition of RNase A. **B:** Immunoprecipitation (IP) was performed using COS-7 cells transiently transfected with $MBNL1_{40}$-myc and YB-1-V5. As indicated by an arrow, MBNL1-myc was present in the YB-1-V5 complex precipitated by anti-V5 antibody. When an RNase A-containing lysis buffer was used, the MBNL1 band was diminished.

was specifically coimmunoprecipitated with YB-1-V5 by anti-V5 antibody. Because these associations diminished when the lysates were pretreated with RNase A (Fig. 2B), it was suggested that these proteins are assembled into RNPs on an RNA scaffold.

α-Actinin Minigene Splicing Assay

Previously, YB-1 was shown to interact with MeCP2 through RNA and to mediate the alternative splicing of CD44 (Young et al., 2005). To investigate the functional interaction between MBNL1 and YB-1, we tested the splicing activity of YB-1 on one of the targets of MBNL1, the α-actinin minigene (Vicente et al., 2007). HEK293 cells were transfected with the minigene and each effector protein plasmid. RT-PCR analysis showed that YB-1 promoted exon skipping, as did MBNL1, although the response was weaker (Fig. 3). It suggests that MBNL1 and YB-1 may cooperate in the alternative splicing of α-actinin. The effect of DDX1 was not significant. We also determined the splicing activity of YB-1 and DDX1 on Clcn1 minigene, but no significant change was observed (data not shown).

Colocalization of MBNL1, YB-1, DDX1, and TIA-1 in HeLa Cells

Although YB-1 affected the splicing of α-actinin, the effect was weak. Combining this with the fact that some ribosomal proteins were identified as MBNL1-binding proteins (Fig. 1), we speculate that the interaction between MBNL1 and YB-1 occurs in the cytoplasm rather than in the nucleus. YB-1 is one of the components of mRNA processing bodies (P-bodies) and stress granules (SGs; Goodier et al., 2007; Yang and Bloch, 2007). Considering that MBNL1 also functions in mRNA metabolism in the cytoplasm, we investigated the localization of GFP-MBNL1 or MBNL1-myc, YB-1-V5, and DDX1-V5 in HeLa cells (Fig. 4). Under normal conditions, MBNL1 and DDX1 localized mainly to the nucleus. On the other hand, nuclear localization of YB-1 was weak. When HeLa cells were subjected to arsenite stress, MBNL1 and YB-1 or DDX1 strongly colocalized to SGs (Fig. 4A,B). CFP-tagged TIA-1, a SGs marker, also colocalized with MBNL1 in SGs (Fig. 4C).

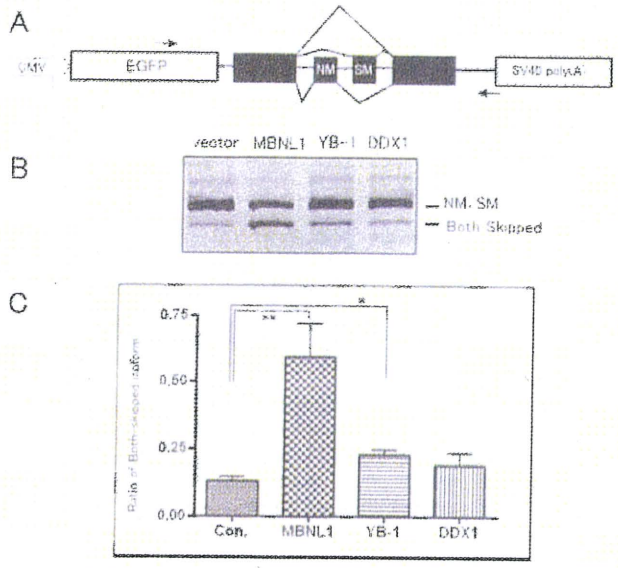

Fig. 3. Splicing of α-actinin by MBNL1. **A:** Diagram of the α-actinin minigene. The sequence of α-actinin containing NM (nonmuscle) and SM (smooth muscle) alternative exons was inserted into the ORF of EGFP-C1. **B:** Upper band indicates NM- or SM-including isoform. Lower band indicates both skipped isoforms. **C:** Quantification of the ratio of both-skipped isoform. When transfected with $MBNL1_{40}$-myc, the both-skipped isoform was promoted. YB-1-V5 also up-regulated the isoform, although less than MBNL1. DDX1-V5 did not significantly affect the splicing. The results are expressed as the mean ± SD of four independent experiments. $*P < 0.05$, $**P < 0.01$.

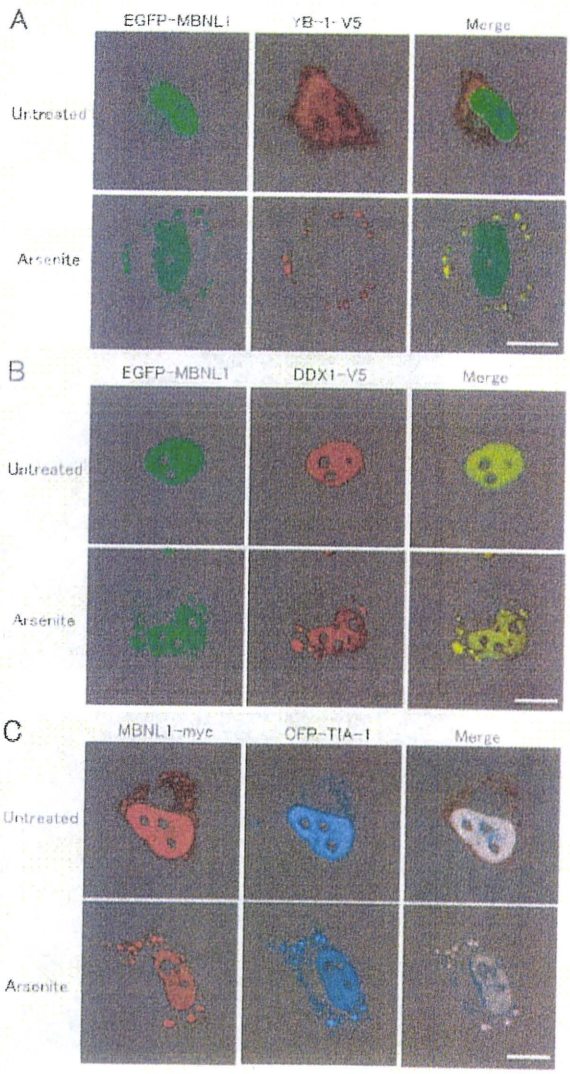

Fig. 4. Colocalization of MBNL1 and YB-1/DDX1 in HeLa. HeLa cells were cotransfected with each pair of expression plasmids. The cells were treated with sodium arsenite (0.5 mM, 45 min) 24 hr after transfection. Cell images were obtained by confocal microscopy. **A:** EGFP-MBNL1 and YB-1-V5 colocalized at cytosolic granules. **B:** DDX1-V5 colocalized with EGFP-MBNL1, as did YB-1-V5. **C:** MBNL1-myc and CFP-TIA-1 were also colocalized, as in A and B. Scale bars = 10 μm.

Production of MBNL1 Polyclonal Antibody and Endogeneous Localization of MBNL1

To investigate the cellular localization of MBNL1, we raised polyclonal antibodies against $MBNL1_{40}$ and observed endogenous MBNL1 localization. The specificity of the antibodies was confirmed by Western blotting (Fig. 5A). Next, using these antibodies, endogenous MBNL1 localization was investigated in COS-7 cells (Fig. 5). Under normal conditions, endogeneous MBNL1 localized mainly to the nucleus. After arsenite treatment, MBNL1 moved to cytoplasmic granules in the cytoplasm and strongly colocalized with TIA-1. It should be noted that MBNL1 also localized to SGs in response to heat stress in HeLa cells as well as in C2C12 myoblasts (data not shown). Therefore, the SG localization of MBNL1 would be a universal phenomenon and should have some physiological functions in SGs.

To examine whether MBNL1 localizes to SGs specifically, we subsequently examined the colocalization of MBNL1 and DCP2, a P-bodies marker. In COS-7 cells transfected with MBNL1-myc and HA-DCP2, colocalization in P-bodies was not detected in response to arsenite stress as well as in normal conditions (Fig. 5B). Thus, we concluded that the MBNL1 granules are mainly SGs, but the possibility that the MBNL1 granules partially overlap with P-bodies cannot be excluded.

YB-1 but Not MBNL1 Associates With Polysomes

Several lines of evidence suggest that YB-1 associates with polysomes (Miwa et al., 2006; Nashchekin et al., 2006). Thus, to investigate further the interaction of MBNL1 and YB-1 in cytoplasmic mRNPs, we per-

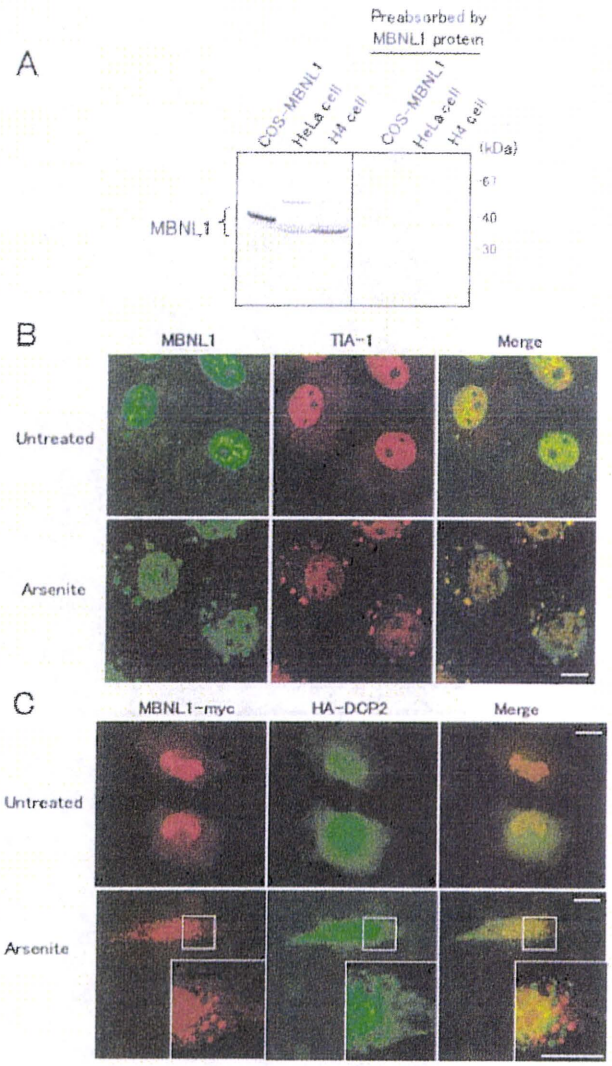

Fig. 5. Endogenous MBNL1 granules in COS-7 cells. **A:** Specificity of polyclonal antibody against MBNL1. Overexpressed $MBNL1_{40}$-myc has a higher molecular weight than that of endogeneous MBNL1 in HeLa or H4 cells. Preabsorption by $MBNL1_{40}$ entirely abolished the staining. **B:** MBNL1 and TIA-1 colocalize endogenously at stress granules after arsenite stress. **C:** MBNL1 granules are distinct from P-bodies. $MBNL1_{40}$-myc and HA-DCP2 were cotransfected into COS-7 cells. The cells were treated with 0.5 mM arsenite for 45 min. Each of the granule types appeared in distinct locations. The MBNL1 granules are larger than those of DCP2. Scale bars = 10 μm.

formed sucrose gradient fractionation. Although YB-1 was found to associate with polysomes, endogenous MBNL1 was not (Fig. 6). Consistent with this result, transiently transfected MBNL1-myc did not associate with polysomes. This suggests that MBNL1 associates with smaller mRNP particles. Our results for MBNL1 are similar to those for Smaug, an mRNA-binding protein that forms SGs like cytoplasmic foci (Baez and Boccaccio 2005). At these foci, Smaug is said to repress the translation of mRNAs. Because YB-1 cofractionated with MBNL1, the interaction of the two proteins may occur in small mRNPs, not in polysomes.

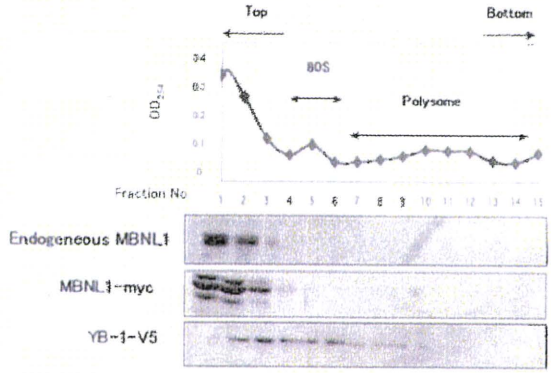

Fig. 6. Polysome analysis. Extracts of HeLa cells that had been incubated with cycloheximide were sedimented through sucrose gradients as described. The polysome and 80S single ribosome sedimentation profiles are shown by A_{254} absorbance. Western blot analysis showed that endogenous MBNL1 was present exclusively in the lighter fractions (lanes 2, 3). YB-1 was present in a broad manner in polysome fractions.

DISCUSSION

The initial aim of this study was to identify MBNL1-binding proteins. We identified several MBNL1-interacting proteins by pull-down and mass spectrometric analyses and subsequently investigated the interaction of MBNL1 with YB-1 and DDX1. YB-1, human Y-box binding protein, belongs to a family of multifunctional nucleic acid-binding proteins. Y-box proteins contain a cold-shock domain (CSD), which is highly conserved, and function as RNA chaperones. YB-1 appears to have roles in RNA splicing (Raffetseder et al., 2003; Young et al., 2005) and translation (Pascual et al., 2006), DNA repair, and transcription (Chernukhin et al., 2000; Klenova et al., 2004; Roberts et al., 2007). Thus, it regulates gene expression at both the transcriptional and the posttranscriptional levels (Pascual et al., 2006).

During the course of our analysis of the interaction between MBNL1 and YB-1, we found that MBNL1 forms SGs in the cytoplasm, like YB-1. Our immunoprecipitation results confirmed that the interaction was mediated by RNA molecules. The two proteins cofractionated in small RNP fractions rather than as polysomes. This suggests that they may form RNP complexes before the bound mRNAs are transported to actively translating ribosomes. We also examined the functional interaction between MBNL1 and YB-1 using an α-actinin minigene splicing assay, and we found that YB-1 weakly promoted SM/NM exon skipping, like MBNL1. Recent reports have described the function of YB-1 in RNA splicing. It

is therefore possible that MBNL1 and YB-1 function cooperatively during splicing.

The DEAD box RNA helicase family is also implicated in RNA splicing (Miller et al., 2000). Although in our system the contribution of DDX1 to alternative splicing could not be detected, it is possible that DDX1 affects the splicing activity of MBNL1 toward other targets. Micro-RNAs (miRNA) are increasingly recognized as major regulators of gene expression in eukaryotes, and DDX1 was recently identified as one of the components of the microprocessor complex (Gregory et al., 2004). It is intriguing to speculate that MBNL1 is also functionally related to miRNA biogenesis. Additionally, DDX1 was demonstrated to associate with cleavage stimulation factor and to be involved in processing the 3′-ends of pre-mRNA molecules (Bleoo et al., 2001). It is possible that MBNL1 is also part of the cleavage body in the nucleus, where it may play a role in constitutive RNA metabolism.

In our study, MBNL1, YB-1, and DDX1 were found to colocalize in the cytoplasm rather than in the nucleus in response to stress. A distinct feature of MBNL1 was its presence in cytosolic foci, and we demonstrated that MBNL1 colocalized with YB-1, DDX1, and TIA-1 at apparent SGs. SGs are discrete cytoplasmic aggregates that can be induced by a variety of stresses, including heat shock, hypoxia, oxidative stress, and viral infections (Anderson and Kedersha, 2002). SGs are considered to be sites of mRNA triage that regulate mRNA stability and translatability. The accumulation of RNAs into dense globules could keep them from reacting with harmful chemicals and safeguard the information that they encode. Molecules can go down one of three paths: storage, degradation, or reinitiation of translation. Recently, it was reported that YB-1, in association with the antiretroviral factor APOBEC3G, relocalizes from P-bodies to SGs when cells are exposed to heat shock stress. Our results show that MBNL1 granules are distinct from P-bodies but that sometimes they are located adjacent to one another. Considering these facts, when a cell is subjected to arsenite stress, YB-1 and MBNL1 colocalized in SGs. Our pull-down screen was not specific for stress conditions; thus, YB-1 and MBNL1 should also interact under normal physiological conditions. Supporting this, the interaction was observed in a nonstressed condition (Fig. 2). Among the proteins identified in our primary screen, the ribosomal protein L7a was identified as a component of SGs (Kim et al., 2006). The ribosomal protein S3 is also a component of SGs (Kedersha et al., 2002). Thus, four of the seven proteins identified in our screen are SGs-related proteins, which strongly suggests that MBNL1 is physiologically related to SGs. Because not all of the ribosomal proteins localized to SGs (e.g., L5 and L37), the components of SGs should be further studied. Investigations of the other MBNL1-interacting proteins as candidate SGs components, such as phenylalaninyl-tRNA synthetase subunits α and β and amylo-1,6-glucosidase, would also be interesting.

The expression of most genes is regulated by multiple mechanisms, and an important control of gene expression is exerted through mRNA stability. The stability of mRNAs is regulated by a variety of signals acting on specific sequences within the RNA. Previously, muscleblind was suggested to play a role in RNA stability in the cytoplasm in *Drosophila* (Houseley et al., 2005). Our data about cytoplasmic dynamics of MBNL1 might support this novel function of muscleblind. In addition, TTP, one of the C_3H zinc finger protein same as muscleblind, was shown either to promote AU-rich element (ARE)-RNA degradation or increase their stability (Houseley et al., 2005). Because TTP is one of the most related genes to MBNL1 in the point of its domain structure, it is reasonable to assume that MBNL1 also has a function in affecting the stability of mRNA in the cytoplasm. Target RNA sequence of MBNL1 is likely to be CHHG (H is A, U, or C) motif (Kino et al., 2004). Because every mRNA should have each specific sequence in 3′-UTR, it is possible that MBNL1 binds to mRNAs, which has a CHHG motif in the 3′-UTR, and controls their RNA stability.

Recently, for the RNA-binding motif protein 4 (RBM4), which plays a regulatory role in alternative splicing of precursor mRNA, it was demonstrated that its functions in translation control are modulated by cell stress (Lin et al., 2007). Although the relation and dynamics between splicing activity and translation control are unknown, it is intriguing to assume that these splicing regulators, including MBNL1, dynamically shuttle between nucleus and cytoplasm in response to cell stress. Further investigation should be done to clarify these splicing regulators dynamics.

In summary, our study demonstrates that MBNL1 formed cytoplasmic SGs and colocalized with YB-1 and DDX1. The functional significance of these events should be investigated further and may lead to a better understanding of the pathogenesis of DM.

ACKNOWLEDGMENTS

We thank Dr. S. Imajoh-Ohmi for mass spectrometry analysis.

REFERENCES

Adereth Y, Dammai V, Kose N, Li R, Hsu T 2005. RNA-dependent integrin alpha3 protein localization regulated by the Muscleblind-like protein MLP1. Nat Cell Biol 7:1240–1247

Allemand E, Hastings ML, Murray MV, Myers MP, Krainer AR. 2007 Alternative splicing regulation by interaction of phosphatase PP2Cgamma with nucleic acid-binding protein YB-1. Nat Struct Mol Biol 14:630–638.

Amack JD, Paguio AP, Mahadevan MS. 1999. Cis and trans effects of the myotonic dystrophy (DM) mutation in a cell culture model. Hum Mol Genet 8:1975–1984.

Anderson P, Kedersha N. 2002. Stressful initiations. J Cell Sci 115:3227–3234.

Artero R, Prokop A, Paricio N, Begemann G, Pueyo I, Mlodzik M, Perez-Alonso M, Baylies MK. 1998. The muscleblind gene participates

in the organization of Z-bands and epidermal attachments of *Drosophila* muscles and is regulated by Dmef2. Dev Biol 195:131–143.

Baez MV, Boccaccio GL. 2005. Mammalian Smaug is a translational repressor that forms cytoplasmic foci similar to stress granules. J Biol Chem 280:43131–43140.

Begemann G, Paricio N, Artero R, Kiss I, Perez-Alonso M, Mlodzik M. 1997. *Muscleblind*, a gene required for photoreceptor differentiation in *Drosophila*, encodes novel nuclear Cys_3His-type zinc-finger-containing proteins. Development 124:4321–4331.

Berul CI, Maguire CT, Aronovitz MJ, Greenwood J, Miller C, Gehrmann J, Housman D, Mendelsohn ME, Reddy S. 1999. DMPK dosage alterations result in atrioventricular conduction abnormalities in a mouse myotonic dystrophy model. J Clin Invest 103:R1–R7.

Bleoo S, Sun X, Hendzel MJ, Rowe JM, Packer M, Godbout R. 2001. Association of human DEAD box protein DDX1 with a cleavage stimulation factor involved in 3′-end processing of pre-MRNA. Mol Biol Cell 12:3046–3059.

Brook JD, McCurrach ME, Harley HG, Buckler AJ, Church D, Aburatani H, Hunter K, Stanton VP, Thirion JP, Hudson T, et al. 1992. Molecular basis of myotonic dystrophy: expansion of a trinucleotide (CTG) repeat at the 3′ end of a transcript encoding a protein kinase family member. Cell 68:799–808.

Chernukhin IV, Shamsuddin S, Robinson AF, Carne AF, Paul A, El-Kady AI, Lobanenkov VV, Klenova EM. 2000. Physical and functional interaction between two pluripotent proteins, the Y-box DNA/RNA-binding factor, YB-1, and the multivalent zinc finger factor, CTCF. J Biol Chem 275:29915–29921.

Cordin O, Banroques J, Tanner NK, Linder P. 2006. The DEAD-box protein family of RNA helicases. Gene 367:17–37.

Davis BM, McCurrach ME, Taneja KL, Singer RH, Housman DE. 1997. Expansion of a CUG trinucleotide repeat in the 3′ untranslated region of myotonic dystrophy protein kinase transcripts results in nuclear retention of transcripts. Proc Natl Acad Sci U S A 94:7388–7393.

Day JW, Ricker K, Jacobsen JF, Rasmussen LJ, Dick KA, Kress W, Schneider C, Koch MC, Beilman GJ, Harrison AR, Dalton JC, Ranum LP. 2003. Myotonic dystrophy type 2: molecular, diagnostic and clinical spectrum. Neurology 60:657–664.

Fardaei M, Larkin K, Brook JD, Hamshere MG. 2001. In vivo colocalisation of MBNL protein with DMPK expanded-repeat transcripts. Nucleic Acids Res 29:2766–2771.

Fardaei M, Rogers MT, Thorpe HM, Larkin K, Hamshere MG, Harper PS, Brook JD. 2002. Three proteins, MBNL, MBLL and MBXL, colocalize in vivo with nuclear foci of expanded-repeat transcripts in DM1 and DM2 cells. Hum Mol Genet 11:805–814.

Fu YH, Friedman DL, Richards S, Pearlman JA, Gibbs RA, Pizzuti A, Ashizawa T, Perryman MB, Scarlato G, Fenwick RG Jr, et al. 1993. Decreased expression of myotonin-protein kinase messenger RNA and protein in adult form of myotonic dystrophy. Science 260:235–238.

Goodier JL, Zhang L, Vetter MR, Kazazian HH Jr. 2007. LINE-1 ORF1 protein localizes in stress granules with other RNA-binding proteins, including components of RNA interference RNA-induced silencing complex. Mol Cell Biol 27:6469–6483.

Gregory RI, Yan KP, Amuthan G, Chendrimada T, Doratotaj B, Cooch N, Shiekhattar R. 2004. The microprocessor complex mediates the genesis of microRNAs. Nature 432:235–240.

Harper PS. 2001. Myotonic dystrophy, 3rd ed.. London: W.B. Saunders.

Ho TH, Charlet BN, Poulos MG, Singh G, Swanson MS, Cooper TA. 2004. Muscleblind proteins regulate alternative splicing. EMBO J 23:3103–3112.

Houseley JM, Wang Z, Brock GJ, Soloway J, Artero R, Perez-Alonso M, O'Dell KM, Monckton DG. 2005. Myotonic dystrophy associated expanded CUG repeat muscleblind positive ribonuclear foci are not toxic to *Drosophila*. Hum Mol Genet 14:873–883.

Jansen G, Groenen PJ, Bachner D, Jap PH, Coerwinkel M, Oerlemans F, van den Broek W, Gohlsch B, Pette D, Plomp JJ, Molenaar PC, Nederhoff MG, van Echteld CJ, Dekker M, Berns A, Hameister H, Wieringa B. 1996. Abnormal myotonic dystrophy protein kinase levels produce only mild myopathy in mice. Nat Genet 13:316–324.

Kanadia RN, Shin J, Yuan Y, Beattie SG, Wheeler TM, Thornton CA, Swanson MS. 2006. Reversal of RNA missplicing and myotonia after muscleblind overexpression in a mouse poly(CUG) model for myotonic dystrophy. Proc Natl Acad Sci U S A 103:11748–11753.

Kedersha N, Chen S, Gilks N, Li W, Miller IJ, Stahl J, Anderson P. 2002. Evidence that ternary complex (eIF2-GTP-tRNA(i)(Met))-deficient preinitiation complexes are core constituents of mammalian stress granules. Mol Biol Cell 13:195–210.

Kim SH, Dong WK, Weiler IJ, Greenough WT. 2006. Fragile X mental retardation protein shifts between polyribosomes and stress granules after neuronal injury by arsenite stress or in vivo hippocampal electrode insertion. J Neurosci 26:2413–2418.

Kino Y, Mori D, Oma Y, Takeshita Y, Sasagawa N, Ishiura S. 2004. Muscleblind protein, MBNL1/EXP, binds specifically to CHHG repeats. Hum Mol Genet 13:495–507.

Klenova E, Scott AC, Roberts J, Shamsuddin S, Lovejoy EA, Bergmann S, Bubb VJ, Royer HD, Quinn JP. 2004. YB-1 and CTCF differentially regulate the 5-HTT polymorphic intron 2 enhancer which predisposes to a variety of neurological disorders. J Neurosci 24:5966–5973.

Kohno K, Izumi H, Uchiumi T, Ashizuka M, Kuwano M. 2003. The pleiotropic functions of the Y-box-binding protein, YB-1. Bioessays 25:691–698.

Lin JC, Hsu M, Tarn WY. 2007. Cell stress modulates the function of splicing regulatory protein RBM4 in translation control. Proc Natl Acad Sci U S A 104:2235–2240.

Liquori CL, Ricker K, Moseley ML, Jacobsen JF, Kress W, Naylor SL, Day JW, Ranum LP. 2001. Myotonic dystrophy type 2 caused by a CCTG expansion in intron 1 of ZNF9. Science 293:864–867.

Mahadevan M, Tsilfidis C, Sabourin L, Shutler G, Amemiya C, Jansen G, Neville C, Narang M, Barcelo J, O'Hoy K, et al. 1992. Myotonic dystrophy mutation: an unstable CTG repeat in the 3′ untranslated region of the gene. Science 255:1253–1255.

Mankodi A, Logigian E, Callahan L, McClain C, White R, Henderson D, Krym M, Thornton CA. 2000. Myotonic dystrophy in transgenic mice expressing an expanded CUG repeat. Science 289:1769–1773.

Mankodi A, Urbinati CR, Yuan QP, Moxley RT, Sansone V, Krym M, Henderson D, Schalling M, Swanson MS, Thornton CA. 2001. Muscleblind localizes to nuclear foci of aberrant RNA in myotonic dystrophy types 1 and 2. Hum Mol Genet 10:2165–2170.

Meola G, Sansone V, Perani D, Scarone S, Cappa S, Dragoni C, Cattaneo E, Cotelli M, Gobbo C, Fazio F, Siciliano G, Mancuso M, Vitelli E, Zhang S, Krahe R, Moxley RT. 2003. Executive dysfunction and avoidant personality trait in myotonic dystrophy type 1 (DM-1) and in proximal myotonic myopathy (PROMM/DM-2). Neuromuscul Disord 13:813–821.

Miller JW, Urbinati CR, Teng-Umnuay P, Stenberg MG, Byrne BJ, Thornton CA, Swanson MS. 2000. Recruitment of human muscleblind proteins to (CUG)(n) expansions associated with myotonic dystrophy. EMBO J 19:4439–4448.

Miwa A, Higuchi T, Kobayashi S. 2006. Expression and polysome association of YB-1 in various tissues at different stages in the lifespan of mice. Biochim Biophys Acta 1760:1675–1681

Nashchekin D, Zhao J, Visa N, Daneholt B. 2006. A novel Ded1-like RNA helicase interacts with the Y-box protein ctYB-1 in nuclear mRNP particles and in polysomes. J Biol Chem 281:14263–14272.

Pascual M, Vicente M, Monferrer L, Artero R. 2006. The Muscleblind family of proteins: an emerging class of regulators of developmentally programmed alternative splicing. Differentiation 74:65–80.

Raffetseder U, Frye B, Rauen T, Jurchott K, Royer HD, Jansen PL, Mertens PR. 2003. Splicing factor SRp30c interaction with Y-box protein-1 confers nuclear YB-1 shuttling and alternative splice site selection. J Biol Chem 278:18241–18248.

Rapp TB, Yang L, Conrad EU 3rd, Mandahl N, Chansky HA. 2002. RNA splicing mediated by YB-1 is inhibited by TLS/CHOP in human myxoid liposarcoma cells. J Orthop Res 20:723–729.

Reddy S, Smith DB, Rich MM, Leferovich JM, Reilly P, Davis BM, Tran K, Rayburn H, Bronson R, Cros D, Balice-Gordon RJ, Housman D. 1996. Mice lacking the myotonic dystrophy protein kinase develop a late onset progressive myopathy. Nat Genet 13:325–335.

Roberts J, Scott AC, Howard MR, Breen G, Bubb VJ, Klenova E, Quinn JP. 2007. Differential regulation of the serotonin transporter gene by lithium is mediated by transcription factors, CCCTC binding protein and Y-box binding protein 1, through the polymorphic intron 2 variable number tandem repeat. J Neurosci 27:2793–2801

Stickeler E, Fraser SD, Honig A, Chen AL, Berget SM, Cooper TA. 2001. The RNA binding protein YB-1 binds A/C-rich exon enhancers and stimulates splicing of the CD44 alternative exon v4. EMBO J 20:3821–3830.

Taneja KL, McCurrach M, Schalling M, Housman D, Singer RH. 1995. Foci of trinucleotide repeat transcripts in nuclei of myotonic dystrophy cells and tissues. J Cell Biol 128:995–1002.

Vicente M, Monferrer L, Poulos MG, Houseley J, Monckton DG, O'Dell K M, Swanson MS, Artero RD. 2007. Muscleblind isoforms are functionally distinct and regulate alpha-actinin splicing. Differentiation 75:427–440.

Yang WH, Bloch DB. 2007. Probing the mRNA processing body using protein macroarrays and "autoantigenomics." RNA 13:704–712.

Young JI, Hong EP, Castle JC, Crespo-Barreto J, Bowman AB, Rose MF, Kang D, Richman R, Johnson JM, Berget S, Zoghbi HY 2005. Regulation of RNA splicing by the methylation-dependent transcriptional repressor methyl-CpG binding protein 2. Proc Natl Acad Sci U S A 102:17551–17558.

Journal of Neuroscience Research 87:1090–1097 (2009)

Identification of *Caenorhabditis elegans* K02H8.1 (CeMBL), a Functional Ortholog of Mammalian MBNL Proteins

Noboru Sasagawa,[1,2]* Eriko Ohno,[1] Yoshihiro Kino,[1,3] Yuichiro Watanabe,[1] and Shoichi Ishiura[1,2]

[1]Department of Life Sciences, Graduate School of Arts and Sciences, University of Tokyo, Tokyo, Japan
[2]Center for Structuring Life Sciences, Graduate School of Arts and Sciences, University of Tokyo, Tokyo, Japan
[3]Laboratory of Structural Neuropathology, Brain Science Institute, RIKEN, Saitama, Japan

The genome of the nematode *Caenorhabditis elegans* possesses an orthologous sequence to the *Drosophila muscleblind* (*mbl*) and mammalian *muscleblind-like* genes (*MBNL*s). This ortholog, K02H8.1, which has a high degree of homology (about 50%) to human *MBNL*s, encodes two zinc finger domains, as does the sequence of the *Drosophila mbl* gene. This distinguishes it from human *MBNL*s, which encode four zinc finger domains. In this study, we cloned six major isoforms of K02H8.1 using cDNA generated from *C. elegans* total RNA. All six of the cloned isoforms had an SL1 leader sequence at the 5′-position. Interestingly, one of the isoforms lacked a zinc finger domain-encoding sequence. To understand better the function of K02H8.1, we performed yeast three-hybrid experiments to characterize the binding of K02H8.1 to bait RNAs. K02H8.1 exhibited strong binding affinity for CUG and CCUG repeats, and the binding affinity was very similar to that of MBNLs. In addition, promoter analysis was performed using promoter-green fluorescent protein (GFP) fusion constructs. The expression of GFP driven by the K02H8.1 promoter was absent in muscle; however, significant GFP expression was detected in the neurons around the pharynx.

Key words: myotonic dystrophy; MBNL; *Caenorhabditis elegans*; CeMBL; K02H8.1

Myotonic dystrophy (dystrophia myotonica, DM) is an autosomal dominant disorder with an incidence of about five individuals per 100,000. DM is one of the most common muscular dystrophies with multisystemic and variable symptoms. The main symptoms are muscle hypertension, myotonia, muscle weakness, cataracts, mental retardation, insulin resistance, heart disorders, gonadal failure, baldness, immunodeficiency, and insulin abnormalities (Harper, 2001).

Two types of DM (type 1 [DM1] and type 2 [DM2]) have been observed, each of which is associated with a different set of mutations. The mutation responsible for DM1 lies within the DM protein kinase (*DMPK*) gene, which is located at chromosomal position 19q13.3 (Brook et al., 1992; Mahadevan et al., 1992). *DMPK* contains a CTG triplet repeat in its 3′-noncoding region; an expansion in the number of repeats has been observed in DM1 patients (Mahadevan et al., 1992). The normal number of CTG repeats is between 5 and 50, whereas hundreds to thousands of repeats have been observed in patients with DM1. Increased numbers of repeats are associated with more severe symptoms and an earlier onset of disease (Tsilfidis et al., 1992).

The mutation responsible for DM2 is located in the *ZNF9* gene, which is found at chromosome position 3q21. This mutation consists of an expansion of CCTG repeats in intron 1 of *ZNF9*. Patients with DM2 have 75–1,000 (or more) of these repeats, whereas 10–27 repeats are considered normal (Liquori et al., 2001).

An interesting feature of DM is that neither DM1 nor DM2 is the result of mutations in the coding regions of *DMPK* or *ZNF9*. Instead, the mutations that give rise to DM are in noncoding regions (i.e., 3′-untranslated region and intron). This indicates that the phenotypes associated with DM are not due to the abnormal function of the translated gene product but are due to the presence of expanded CUG or CCUG repeats within the transcript. There is evidence that the production of a transcript containing an expanded CUG or CCUG repeat is the molecular basis of DM1 and DM2, and this evidence is based on the interaction of repeat sequences with the protein CUG-BP1 and MBNLs. CUG-BP1 (originally named *CUG triplet-binding protein*) was first

The first two authors contributed equally to this work.

Contract grant sponsor: Ministry of Health, Labor, and Welfare, Japan.

*Correspondence to: Noboru Sasagawa, Department of Life Sciences, Graduate School of Arts and Sciences, University of Tokyo, Tokyo 153-8902, Japan. E-mail: sasagawa@csls.c.u-tokyo.ac.jp

Received 27 June 2008; Revised 17 August 2008; Accepted 24 September 2008

Published online 19 November 2008 in Wiley InterScience (www.interscience.wiley.com). DOI: 10.1002/jnr.21942

reported to bind the CUG repeat sequence in RNA (Timchenko et al., 1996; Begemann et al., 1997). However, recent evidence suggests that CUG-BP1 does not in fact bind to CUG repeats but instead to a UG dinucleotide repeat (Takahashi et al., 2000; Kino et al., 2004; Mori et al., 2008). Muscleblind-like 1 (MBNL1) was first identified as a CUG repeat-binding protein in UV cross-linking experiments. Muscleblind-like proteins (MBNLs) colocalize with CUG or CCUG repeat foci in the cells of DM1 and DM2 patients (Miller et al., 2000). MBNL1 plays an important role in the splicing of cardiac troponin T (*cTNT*; Ho et al., 2004) and insulin receptor (*IR*; Savkur et al., 2001). The aberrant splicing of genes such as those encoding muscle-specific chloride channel (*Clcn1*; Charlet-B et al., 2002) and IR has been observed in DM patients, as has the increased expression of CUG-BP1 (Savkur et al., 2001). *Mbnl1* overexpression rescues the disease-associated phenotypes in CUG repeat-overexpressing mice (Kanadia et al., 2006). We previously showed that the level of transcription of CUG-BP1 in DM patients was equal to that in non-DM controls by using real-time PCR (Nezu et al., 2007). This indicates that the increased expression of CUG-BP1 is a posttranscriptional event.

Studies on the localization of MBNLs have found that they colocalize with repeat RNA foci in fibroblasts from DM1 and DM2 patients (Fardaei et al., 2002). Such foci have also been observed at neuromuscular junctions in DM1 patients (Wheeler et al., 2007). MBNL1, MBNL2, and MBNL3 have all been observed in nuclear foci. Although these foci and splicing abnormalities are thought to be independent (Ho et al., 2005a), MBNL could play an important role in DM pathogenesis. In addition, MBNL1 actually binds to the intron of cTNT (Yuan et al., 2007).

The overexpression of an expanded CUG repeat in *Drosophila* results in developmental abnormalities of the eye; however, the expression levels of CUG-BP1 and MBNLs affect the phenotype induced by CUG expansion (de Haro et al., 2006). A possible explanation for this is that MBNL1 and CUG-BP function together in splicing and RNA processing. CUG-BP1 transgenic mice show splicing abnormalities in genes such as those encoding cTNT, myotubularin-related 1, and Clcn1 (Ho et al., 2005b). MBNL1 knockout mice exhibit cataracts and muscular abnormalities (Kanadia et al., 2003a), similar to DM patients. Moreover, the mice show abnormal splicing of *cTNT*, *Clcn1*, and *TNNT3*. Taken together, these results indicate that the abnormal splicing of these genes is due to a loss of function of MBNL1 or the overexpression of CUG-BP1. Recently, the involvement of MBNL1 in stress granules was reported (Onishi et al., 2008).

As a model organism, *Caenorhabditis elegans* has many advantages. One major challenge we faced in this work was to establish *C. elegans* as a model for studying the molecular basis of DM. In *C. elegans*, the K02H8.1 gene (a predicted ortholog of human *MBNLs*) is located on the X chromosome. We cloned *C. elegans* K02H8.1 and functionally identified it as *C. elegans muscleblind* (*CeMBL*).

MATERIALS AND METHODS

Breeding of *C. elegans*

C. elegans strain N2 was used in this study. The deletion mutant Tm1563 was kindly provided by Dr. S. Mitani (Tokyo Women's Medical University, Tokyo, Japan). Nematode growth medium (NGM)-containing plates and *E. coli* strain OP50 were used to breed the nematodes as previously described (Brenner, 1974).

cDNA Cloning

Nematodes contained in a 6-cm dish were washed with M9 buffer and collected into microfuge tubes. They were then centrifuged, and the supernatant was removed. RNA was extracted using Trizol (Gibco BRL, Grand Island, NY) or Isogen (Nippongene) according to the manufacturers' instructions. Reverse transcription reactions to generate cDNA were carried out with Superscript II (Invitrogen, La Jolla, CA) with 250 ng of total RNA and 250 ng of oligo(dT).

The synthesized cDNA was used as the template for PCR. mRNA molecules in *C. elegans* have an SL1 or SL2 leader sequence at their 5′-end, so SL1 (5′-GGTTTAATTACCCAAGTTTGAG-3′) or SL2 (5′-GGTTTTAACCCAGTTACTCAAG-3′) was used as the forward primer. For the reverse primer, we designed two sequences for nested PCR: 5′-ATTATGAGAGAGAGAGAGGAATGTGTGT-3′ (nest1) and 5′-CTAGAATGGTGGTGGCTGCATGTACTCAC-3′ (nest2). The products were ligated into pGEM-T Easy. The Beckman CEQ-8000 system was used to sequence the cloned inserts. To study the expression pattern of each K02H8.1 isoform during development, we first amplified the DNA using primers SL1 and nest1 and then performed a second round of PCR using an exon 3-specific primer (5′-ATGTTCGACGAAAACAGTAATGCCGCTGG-3′) and nest2. Each product was confirmed by sequencing.

Yeast Three-Hybrid System

The budding yeast *Saccharomyces cerevisiae* L40-coat strain and the vector pIIIA/MS2-2 were kind gifts from Dr. M. Wickens (University of Wisconsin). The prey vector used was pACT2 AD (Clontech, Logan, UT). Standard two-hybrid protocols were used for the transformation and maintenance of the yeast. Constructs with repeat regions of various lengths were cloned into pIIIA/MS2-2. K02H8.1s (CeMBLs) was cloned into pACT2 AD. The constructs were then transformed into *S. cerevisiae* L40-coat strain and grown on synthetic dextrose (SD) plates without leucine and uracil. For the histidine plate assay, SD plates without leucine, uracil, and histidine were used. For the histidine assay, 0, 0.1, 0.5, or 1.0 mM 3-amino-1,2,4-triazole (3-AT), which is a competitive inhibitor of histidine synthesis, was added to the plates. For the quantitative β-galactosidase assay, chlorophenol red β-D-galactopyranoside (CPRG) was used as the substrate. To construct a deletion mutant of CeMBL, we used the following primers: 5′-ATGTTCGACGAAAACAGTAATGCCGCTG

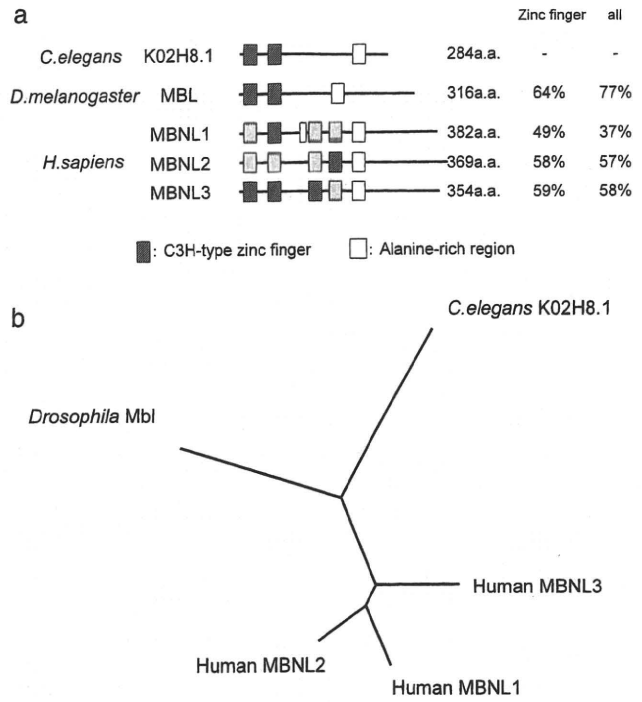

Fig. 1. Sequence similarity among the *C. elegans* K02H1.8, *Drosophila* muscleblind, and human muscleblind-like protein families. **a:** Hatched boxes denote C3H-type zinc finger domains; open boxes denote alanine-rich elements. The sequence homology scores of the C3H-type zinc finger domains and full-length proteins are shown. **b:** Phylogenetic tree for the human MBNL1–3, *Drosophila* muscleblind, and *C. elegans* K02H8.1 proteins created with ClustalX software.

G-3′ (forward) and 5′-CTCGAGCATTGGAGTTCCAGTC TGATTAAG-3′ (reverse).

Life Span Analysis

N2 and Tm1563 nematodes were cultured in 6-cm NGM plates with *Escherichia coli* OP50. We used an adult nematode that laid eggs overnight and then removed the adult from the plate in the morning. We defined time zero as the point at which the eggs hatched. Eggs and L1–3 larvae were grown at 15°C and then transferred to 25°C at the L4 and adult stages.

Promoter Analysis Based on GFP Expression

The promoter region of the gene was cloned from the wild-type *C. elegans* genome by PCR using the following primers: forward, 5′-AACTGCAGGTGCAATGGGCTACT GATCTCC-3′ and reverse, 5′-CGGGATCCCATTCCGT CACTTGCAAAGAAC-3′. Each primer contained an additional PstI and BamHI site, respectively. The resulting fragment was ligated into pPD95.75 (kindly provided by Dr. A. Fire, Stanford School of Medicine) using the PstI and BamHI sites. The resulting plasmid, K02H8.1pro::GFP, was mixed with pRF4, which contains the marker *rol-6* (su1006). The ratio of K02H8.1pro::GFP to pRF4 in the mixed solution was between 1:1 and 1:4. All twisted F1 transformants were collected, and the F3 or later transformants were analyzed by fluorescence microscopy (IX70; Olympus).

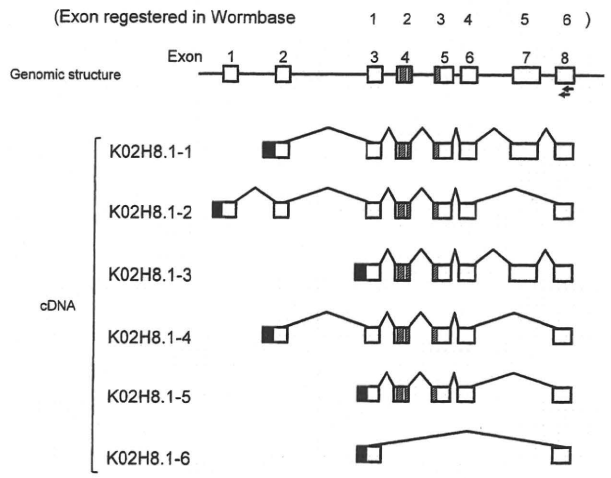

Fig. 2. Cloning of K02H8.1 from cDNA. Open boxes indicate exons; hatched boxes indicate C3H-type zinc finger domains; solid boxes indicate the SL1 leader sequences. Arrowheads in the genomic structure represent the reverse primers used for nested PCR. Six major isoforms of K02H8.1 were identified, including new exons that were not registered in Wormbase. These exons were named *exon 1* and *exon 2*, and the remaining exons were renumbered to reflect this.

RESULTS

Cloning of K02H8.1

K02H8.1 (NCBI accession No. NM078345; Wormbase WBGene00019347) was identified through an in silico search of databases to find a gene with a high degree of homology to human *MBNLs*. K02H8.1, which is located on chromosome X of the *C. elegans* genome, has a high level of homology to the *Drosophila mbl* gene (77%) and human *MBNLs* (37–58%) on the amino acid level (Fig. 1a). There are three *MBNL* loci in the human genome, but only one locus with significant sequence similarity was found in the *C. elegans* genome. Figure 1b shows a phylogenetic tree for human MBNL1–3, *Drosophila* Mbl, and *C. elegans* K02H8.1 proteins. As shown, MBNL3 has the highest similarity to K02H8.1 among the human MBNL1–3 proteins. *MBNL3* may be the ancestral gene for all human *MBNLs*. It is interesting that both MBNL3 and K02H8.1 are located on the X chromosome, whereas *Drosophila mbl* is located on chromosome 2, human *MBNL1* is located on chromosome 3, and *MBNL2* is located on chromosome 13. After the identification of sequences with a high level of similarity to *Drosophila mbl* and human *MBNLs*, we cloned K02H8.1 from *C. elegans* cDNA by PCR using the primers SL1 or SL2 (forward) and a K02H8.1-specific primer (reverse). Using SL1 as the forward primer, six major isoforms of K02H8.1 (Fig. 2) were amplified, whereas using SL2 as the forward primer resulted in no PCR products. This

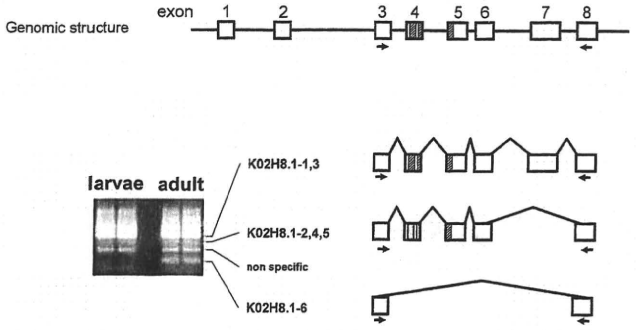

Fig. 3. Expression pattern of K02H8.1 at different developmental stages, showing our nested PCR results (see Materials and Methods). The primers used in the second round of PCR are indicated by arrowheads. K02H8.1-3 and -5 appear in the same band, and K02H8.1-2, -4, and -5 appear in the same band. The K02H8.1-6 product can be seen in the adult sample but not in the larval sample.

indicates that the SL1 leader sequence is added to all K02H8.1 transcripts. In *C. elegans*, many genes are transcribed as a single polycistronic RNA that is subsequently processed, giving rise to multiple mRNAs. The SL1 leader sequence is added to the first of these mRNAs, whereas the SL2 sequence is added to the second and all subsequent mRNAs. Therefore, our result indicates that the expression of each K02H8.1 isoform is regulated by its own upstream promoter.

The six isoforms of K02H8.1 were named K02H8.1-1 to K02H8.1-6. The expression of each isoform of K02H8.1 was analyzed by RT-PCR, and the results show a significant change in the expression of these splicing isoforms during development. No fragment for K02H8.1-6 was observed on a plate containing L1–4 larvae; however, a significant band was obtained from a sample prepared at the adult stage (Fig. 3).

Binding Affinity of K02H8.1 for RNA Containing Repeated Sequences

To examine the RNA binding function of K02H8.1, we performed a yeast three-hybrid analysis. An outline of the assay is shown in Figure 4a. We used K02H8.1-3 and K02H8.1-5 as prey and various repeat RNAs as bait. Reporter genes allowing the yeast to survive on plates without histidine are activated only when the bait RNA and prey protein bind. 3-AT, a competitive inhibitor of histidine synthesis, was used to eliminate false positives.

The results of the histidine assay in Figure 4 are summarized in Table I. As shown, the K02H8.1 isoforms containing zinc fingers had a pattern of RNA binding similar to that of human MBNL1; the sequences $(CUG)_{21}$ and $(CCUG)_{22}$ in particular had higher binding affinities, whereas $(CUUG)_{38}$ and $(CCCG)_{21}$ also exhibited significant binding. Interestingly, the binding affinity of the longer repeats, which correlate to DM, was similar to that of human MBNL1. In contrast, K02H8.1 (-3 and -5) and MBNL1 had different binding

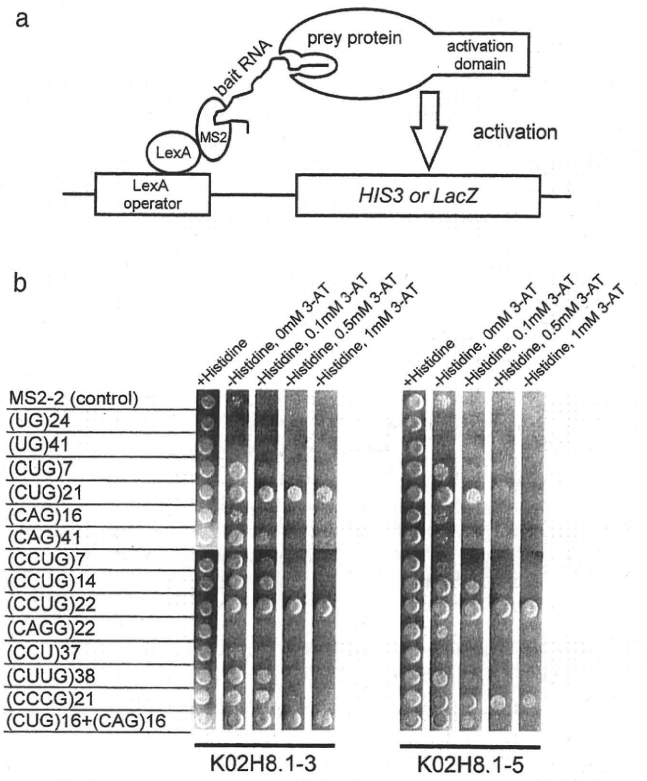

Fig. 4. **a:** Outline of the yeast three-hybrid approach. K02H8.1 was used as prey, and several RNA repeats were used as bait. The diagram is a modified version of that in SenGupta et al. (1996). **b:** Results of the yeast three-hybrid histidine assay. Transformants were seeded to test their viability on the selection plates lacking histidine but containing 0, 0.1, 0.5, or 1 mM 3-amino triazole (3-AT).

TABLE I. Summary of the Binding Affinities Between K02H8.1s and Various Repeat RNAs in Our Yeast Three-Hybrid System (Histidine Assay)

	K02H8.1-3	K02H8.1-5	MBNL1
MS2–2 (control)	–	–	–
$(UG)_{24}$	–	–	–
$(UG)_{41}$	–	–	n.t.
$(CUG)_7$	–	–	–
$(CUG)_{21}$	++++	+++	+++
$(CAG)_{16}$	–	–	++
$(CAG)_{41}$	+++	–	++
$(CCUG)_7$	++	–	–
$(CCUG)_{14}$	+++	+++	n.t.
$(CCUG)_{22}$	+++++	+++++	++++
$(CAGG)_{22}$	–	–	–
$(CCU)_{37}$	–	–	–
$(CUUG)_{38}$	+++	+	+++
$(CCCG)_{21}$	+++	++++	++++
$(CUG)_{16}$ + $(CAG)_{16}$	++++	++	–

*The viability of the transformants was classified as follows: +++++, ++++, +++, and ++ were viable in the presence of 1.0, 0.5, 0.1, and 0 mM 3-AT, respectively; + indicates growth in the absence of 3-AT (0 mM) after more than 1 week; – indicates no viability in the presence of 0 mM 3-AT. False positives in MS2-2 (control) were taken into account to estimate the relative viabilities. The survival rates for MBNL1 are taken from Kino et al. (2003). n.t., Not tested.

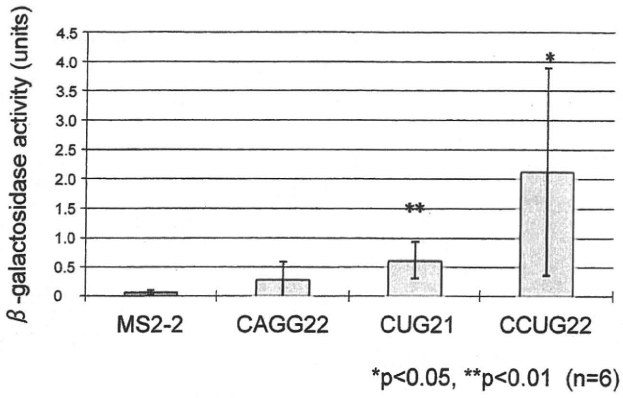

Fig. 5. Yeast three-hybrid system and β-galactosidase assay (K02H8.1-5). Yeast transformants were incubated in synthetic liquid medium, and the cells were harvested by centrifugation. The formation of a colored product was assessed based on the absorbance. β-Galactosidase activity [in units (U)] was calculated as follows: $U = 1{,}000 \times OD_{578}/(t \times V \times OD_{600})$, where t = incubation time and V = reaction volume.

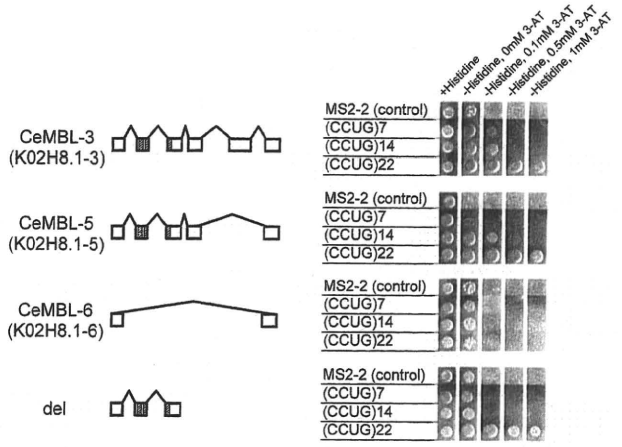

Fig. 6. Yeast three-hybrid assay of CeMBL-3, -5, and -6 and the CeMBL deletion mutant (del). Transformants were seeded to test their viability on the selection plates as described for Figure 4b.

affinities for the sequences $(CAG)_{16}$ and $(CUG)_{16} + (CAG)_{16}$ (double-stranded), indicating that K02H8.1 does not exactly match the binding specificity of human MBNL1. Moreover, K02H8.1-3 and K02H8.1-5 showed slightly different binding preferences for $(CAG)_{41}$, $(CUUG)_{38}$, and $(CCUG)_7$. In particular, K02H8.1-3 had an affinity for $(CAG)_{41}$, whereas K02H8.1-5 did not.

To quantitate the binding affinities of the K02H8.1 proteins for the bait RNAs, β-galactosidase assays were performed (K02H8.1-5). As shown by our results, the repeat sequences $(CUG)_{21}$ and $(CCUG)_{22}$ had significant binding affinities compared with the negative controls ($P < 0.05$; Fig. 5). These data clearly show that K02H8.1 has both functional and structural similarity to human MBNLs. Therefore, we determined that K02H8.1 is an ortholog of human *MBNLs* and renamed it *C. elegans muscleblind* (*CeMBL*). The isoforms of K02H8.1 (-1 to -6) were renamed CeMBL-1 to -6.

The next question was whether the RNA-binding motif of CeMBL is required for RNA binding. An analysis of the CeMBL-6 isoform, a splicing variant lacking the zinc finger RNA-binding motif, suggested that the motif is required. CeMBL-6 did not bind RNAs containing a CCUG repeat in our yeast three-hybrid system. In addition, a deletion mutant lacking the C-terminus (i.e., possessing only the N-terminal domain and RNA-binding motif) showed significant binding affinity for CCUG repeats. However, this affinity was weaker than that of CeMBL-3 and -5, especially for shorter CCUG repeats, such as $(CCUG)_{14}$. These results indicate that C3H-type zinc finger domains are necessary for CeMBL RNA binding activity (Fig. 6, Table II).

TABLE II. Binding Affinities of CeMBLs and a CeMBL Deletion Mutant for RNAs Containing CCUG Repeats in Our Yeast Three-Hybrid System (Histidine Assay)

	CeMBL-3 (K02H8.1-3)	CeMBL-5 (K02H8.1-5)	CeMBL-6 (K02H8.1-6)	del
MS2-2 (control)	–	–	–	–
$(CCUG)_7$	++	–	–	–
$(CCUG)_{14}$	+++	+++	–	–
$(CCUG)_{22}$	+++++	+++++	–	+++++

The viability of the transformants was assessed as in Table I.

Analysis of a *CeMBL* Mutant

The *CeMBL* mutant Tm1563 has a deletion in exon 3 and in the introns around exon 3. The deletion of these regions was confirmed by sequencing of the PCR-amplified *CeMBL* region from the Tm1563 genome. Our sequence data showed a 513-bp deletion and a 2-bp insertion around exon 1 in *CeMBL*. These mutations cause a frameshift at exon 2, resulting in a lack of RNA-binding motifs within the CeMBL protein.

The Tm1563 mutant did not appear to have abnormal development or behavior; however, it did have a shorter life span (Fig. 7): 14.2 ± 0.77 days (n = 20) compared with 18.5 ± 1.40 days (n = 16) for the wild type.

Promoter Analysis of *CeMBL*

To determine the expression pattern of *CeMBL*, a genomic clone containing the 2.4-kb region upstream of *CeMBL* exon 1, an intermediate intron, and part of exon 2 was used. A fusion construct was made using the *CeMBL* fragment from this clone and pTD95.77; the resulting plasmid had an in-frame fusion of *CeMBL* exon 2 and GFP. This fusion construct was then injected into nematodes harboring the *rol-6* marker.

Analysis of GFP expression in the nematodes showed fluorescence in the excretory cell, seminal vesicle, and nerve cells that run parallel to the pharynx and body axis (Fig. 8). GFP expression was observed at all developmental stages, including egg, L1–L4, and adult,

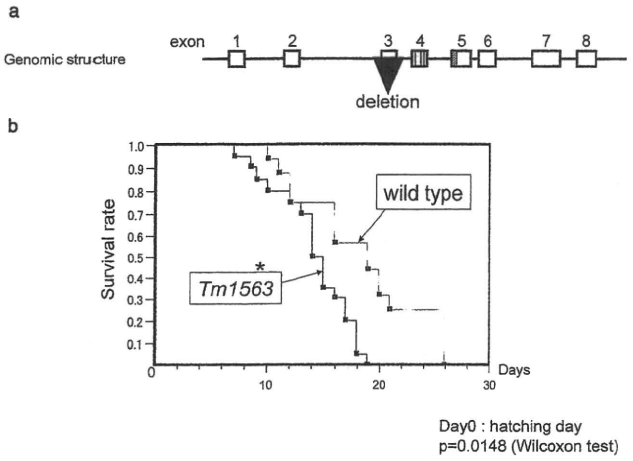

Fig. 7. Life span analysis of a *CeMBL* mutant. **a:** Diagram of the structure of *CeMBL* in Tm1563. **b:** The survival rates for Tm1563 and wild-type strain N2 are plotted.

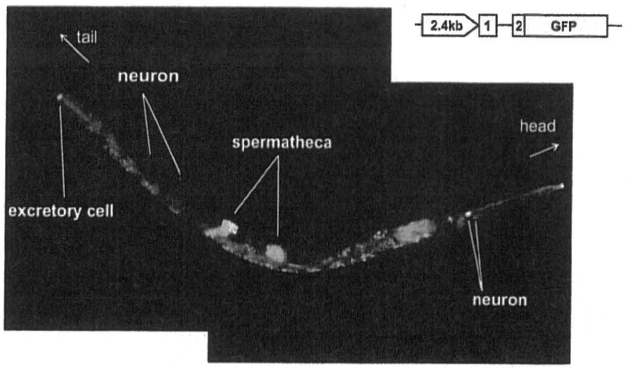

Fig. 8. Promoter analysis of *CeMBL*. GFP expression was observed in the excretory cell, seminal vesicle, and nerve cells that run parallel to the pharynx and body axis.

suggesting that *CeMBL* expression occurs during the early stages of development.

DISCUSSION

Our results clearly show that K02H8.1 (*CeMBL*) is a functional ortholog of *Drosophila mbl* and human *MBNLs*. The *Drosophila mbl* mutant was first identified from its dysfunctional eye development. A recent report showed that *mbl* has several splicing isoforms that are involved in the alternative splicing of α-actinin (Vicente et al., 2007). Several splicing isoforms of *MBNLs* have been reported in humans (Miller et al., 2000). In our experiments, we found several splicing isoforms of *CeMBL* in *C. elegans*. One of these isoforms, K02H8.1-6 (CeMBL-6), was of particular interest, because as we saw no expression in larvae but significant expression in adults (Fig. 3). K02H8.1-6 (CeMBL-6) does not have a zinc finger domain, suggesting that it does not bind RNA. Human MBNLs also have an isoform that lacks a zinc finger, but the physiological function of this isoform is unknown.

A major challenge in this work was the identification of K02H8.1 as a functional ortholog of human *MBNLs*. The results of our yeast three-hybrid experiments suggested that the binding affinity of K02H8.1 for RNA containing repeat sequences is comparable to that of human MBNLs, indicating that K02H8.1 is orthologous to human *MBNLs*. In these experiments, we observed that K02H8.1 (*CeMBL*) bound CUG, CUUG, CCCG, and (especially) CCUG repeats (Fig. 4, Table I), which are also known to be target sequences for human MBNLs. Interestingly, the CeMBL protein possesses only two zinc fingers compared with the four zinc fingers found in human MBNLs, yet these proteins have similar binding specificities for sequences containing repeats. This suggests that the binding preference of CeMBL-family proteins for RNA molecules containing repeat sequences is not determined by the number of zinc fingers within the protein; however, variation in the number of zinc fingers may explain the small differences in affinity of human MBNLs and CeMBL for certain sequences, such as $(CUG)_{16}$ + $(CAG)_{16}$. Actually, MBNLs bind the intron of *cTNT*, and the binding sequence has been determined (Warf and Berglund, 2007). One interesting finding is that splicing abnormalities can be overcome by the overexpression of MBNLs, and increases in MBNL expression have been shown to restore a normal splicing pattern (Kanadia et al., 2006).

Significant binding was observed between CeMBL-3 and the $(CAG)_{41}$ repeat, similarly to human MBNL1. Human MBNL1 forms nuclear foci with both CTG and CAG repeats (Ho et al., 2005a). Although the coexpression of MBNL1 with a long CAG repeat does not affect the splicing of *cTNT* or *IR* (Ho et al., 2005a), the binding affinities of CeMBL and MBNL1 for CAG repeats may have important physiological consequences.

Moreover, binding to the $(CAG)_{41}$ repeat occurred only with CeMBL-3, and not CeMBL-5. The only difference between CeMBL-3 and -5 is an insertion of exon 7. Thus, exon 7, which is located at the C-terminus, may regulate the binding preference of CeMBL. The altered binding affinity of the deletion mutant for molecules containing a CCUG repeat (Fig. 6, Table II) supports the idea that the C-terminal domain (exons 6–8) regulates the RNA binding preferences of CeMBL.

As part of this work, we investigated the *CeMBL* mutant Tm1563. Tm1563 has a mutation in exon 3 of *CeMBL*, upstream of the RNA-binding motif. The result of this mutation is a CeMBL protein that lacks the ability to bind RNA. An analysis of the phenotype of this mutant showed that it had a reduced life span compared with wild-type *C. elegans* (Fig. 7), a finding that is supported by RNAi experiments (Wang et al., 2008) showing that the inhibition of CeMBL expression also resulted in a shorter life span in *C. elegans*.

The mechanism by which the inactivation of *CeMBL* leads to a reduced life span is currently unknown. One possible explanation is the effect on the level of oxidative stress, which is an important factor in

aging. Oxidative stress results in damage to DNA, proteins, and fatty acids. We previously reported that the expression of a longer CTG repeat sequence in cultured C2C12 mouse cells increased cellular sensitivity to oxidative stress (Takeshita et al., 2003). Therefore, the shorter life span of *C. elegans* with inactivated *CeMBL* may be due to splicing abnormalities in certain genes involved in oxidative stress.

Previous experiments indicated that the mRNA expression of MBNLs and CELF was similar in DM patients and non-DM controls (Nezu et al., 2007). This indicates that MBNL function might be controlled at the protein level. The shorter life span associated with the inactivation of *CeMBL* is significant, especially in comparison with the phenotype of MBNL knockout mice, which exhibit DM symptoms and splicing abnormalities. Nevertheless, additional biochemical studies are needed to investigate the role of CeMBL in determining life span.

We also analyzed the location of CeMBL expression by comparing tissues in which MBNLs and Mbl are expressed. Human MBNL1 was expressed mainly in skeletal muscle, heart, brain, intestine, kidney, liver, lung, and placenta. The tissues in which MBNL2 was expressed were largely the same, although the level of expression in skeletal muscle was not as high. MBNL3 expression occurs mainly in the placenta, but is also seen at very low levels in the heart, liver, kidney, and intestine (Kanadia et al., 2003b). MBNL3 (also known as CHCR) inhibits myogenic differentiation (Squillace et al., 2002; Lee et al., 2008). Moreover, the expression of MBNL decreases over the course of differentiation (Lee et al., 2007). In *Drosophila*, Mbl expression has been reported in the eye, central nervous system, and most muscle types, in accordance with the fact that the disruption of *Drosophila mbl* leads to changes in photoreceptor differentiation (Begemann et al., 1997). To analyze the location of CeMBL expression in *C. elegans*, we used the DNA sequence upstream of *CeMBL* fused to GFP. In these experiments, GFP fluorescence was seen in the excretory cell, in the seminal vesicle, and in the nerve cells that run parallel to the pharynx and body axis. No GFP fluorescence was seen in muscle tissue (Fig. 8).

Analysis of the expression of CeMBL in neurons showed comparable levels in *C. elegans*, *Drosophila*, and human, whereas expression was absent in muscle, unlike the case in *Drosophila* and human. There are several explanations for the lack of expression in muscle in *C. elegans*. One is that CeMBL has six splicing variants, and it is possible that each of these isoforms has a unique expression pattern. There is a large intron between exons 2 and 3 (~12 kb) in the *CeMBL* genomic structure, which may contain a *cis* element that affects the expression of the gene. Another is that in silico analysis indicated putative promoter elements in the 3-kb region upstream of exon 3 (i.e., in the 12-kb intron; data not shown). Therefore, it is possible that the expression of *CeMBL* is regulated by multiple promoter sequences.

In conclusion, our study clearly indicates that CeMBL has remarkable similarities to MBNL, not only in terms of its structure but also in terms of its RNA-binding capacity. The physiological functions of CeMBL and MBNL, including RNA splicing, may be highly conserved between species.

ACKNOWLEDGMENTS

We thank Prof. Marvin Wickens for providing the yeast three-hybrid samples, Prof. Shohei Mitani for providing Tm1563, Prof. Andrew Fire for providing vectors, and Prof. Yuichi Iino for helpful advice concerning *C. elegans*.

REFERENCES

Begemann G, Paricio N, Artero R, Kiss I, Prez-Alonso M, Mlodzik M. 1997. *muscleblind*, a gene required for photoreceptor differentiation in *Drosophila*, encodes novel nuclear Cys3His-type zinc-finger-containing proteins. Development 124:4321–4331.

Brenner S. 1974. The genetics of *Caenorhabditis elegans*. Genetics 77: 71–94.

Brook JD, McCurrach ME, Harley HG, Buckler AJ, Church D, Aburatani H, Hunter K, Stanton VP, Thirion JP, Hudson T, Sohn R, Zemelman B, Snell RG, Flundle SA, Crow S, Davies J, Shelbourne P, Buxton J, Jones C, Juvonen V, Johnson K, Harper PS, Shaw DJ, Housman DE. 1992. Molecular basis of myotonic dystrophy: expansion of a trinucleotide (CTG) repeat at the 3′ end of a transcript encoding a protein kinase family member. Cell 68:799–808.

Charlet-B N, Savkur RS, Singh G, Philips AV, Grice EA, Cooper TA. 2002. Loss of the muscle-specific chloride channel in type 1 myotonic dystrophy due to misregulated alternative splicing. Cell 10:45–53.

de Haro M, Al-Ramahi I, De Gouyon B, Ukani L, Rosa A, Faustino NA, Ashizawa T, Cooper TA, Botas J. 2006. MBNL1 and CUGBP1 modify expanded CUG-induced toxicity in a *Drosophila* model of myotonic dystrophy type 1. Hum Mol Genet 15:2138–2145.

Fardaei M, Rogers MT, Thorpe HM, Larkin K, Hamshere MG, Harper PS, Brook JD. 2002. Three proteins, MBNL, MBLL and MBXL, co-localize in vivo with nuclear foci of expanded-repeat transcripts in DM1 and DM2 cells. Hum Mol Genet 11:805–814.

Harper PS. 2001. Myotonic dystrophy,3rd ed. Philadelphia: W.B. Saunders.

Ho TH, Charlet-B N, Poulos MG, Singh G, Swanson MS, Cooper TA. 2004. Muscleblind proteins regulate alternative splicing. EMBO J 23:3103–3112.

Ho TH, Savkur RS, Poulos MG, Mancini MA, Swanson MS, Cooper TA. 2005a. Colocalization of *muscleblind* with RNA foci is separable from mis-regulation of alternative splicing in myotonic dystrophy. J Cell Sci 118:2923–2933.

Ho TH, Bundman D, Armstrong DL, Cooper TA. 2005b. Transgenic mice expressing CUG-BP1 reproduce splicing mis-regulation observed in myotonic dystrophy. Hum Mol Genet 14:1539–1547.

Kanadia RN, Johnstone KA, Mankodi A, Lungu C, Thornton CA, Esson D, Timmers AM, Hauswirth WW, Swanson MS. 2003a. A *muscleblind* knockout model for myotonic dystrophy. Science 302:1978–1980.

Kanadia RN, Urbinati CR, Crusselle VJ, Luo D, Lee YJ, Harrison JK, Oh SP, Swanson MS. 2003b. Developmental expression of mouse *muscleblind* genes *Mbnl1*, *Mbnl2* and *Mbnl3*. Gene Express Patterns 3:459–462.

Kanadia RN, Shin J, Yuan Y, Beattie SG, Wheeler TM, Thornton CA, Swanson MS. 2006. Reversal of RNA missplicing and myotonia after *muscleblind* overexpression in a mouse poly (CUG) model for myotonic dystrophy. Proc Nat Acad Sci U S A 103:11748–11753.

Kino Y, Mori D, Oma Y, Takeshita Y, Sasagawa N, Ishiura S. 2004. Muscleblind protein, MBNL1/EXP, binds specifically to CHHG repeats. Hum Mol Genet 13:495–507.

Lee KS, Squillace RM, Wang EH. 2007. Expression pattern of *muscleblind*-like proteins differs in differentiating myoblasts. Biochem Biophys Res Commun 361:151–155.

Lee KS, Smith K, Amieux PS, Wang EH. 2008. MBNL3/CHCR prevents myogenic differentiation by inhibiting MyoD-dependent gene. Differentiation 76:299–309.

Liquori CL, Ricker K, Moseley ML, Jacobsen JF, Kress W, Naylor SL, Day JW, Ranum LP. 2001. Myotonic dystrophy type 2 caused by a CCTG expansion in intron 1 of ZNF9. Science 293:864–867.

Mahadevan M, Tsilfidis C, Sabourin L, Shutler G, Amemiya C, Jansen G, Neville C, Narang M, Barcel J, O'Hoy K, Lebond S, Earle-Macdonald J, de Jong PJ, Wieringa B, Korneluk RG. 1992. Myotonic dystrophy mutation: an unstable CTG repeat in the 3′ untranslated region of the gene. Science 255:1253–1255.

Miller JW, Urbinati CR, Teng-Umnuay P, Stenberg MG, Byrne BJ, Thornton CA, Swanson MS. 2000. Recruitment of human *muscleblind* proteins to (CUG)(n) expansions associated with myotonic dystrophy. EMBO J 19:4439–4448.

Mori D, Sasagawa N, Kino Y, Ishiura S. 2008. Quantitative analysis of CUG-BP1 binding to RNA repeats. J Biochem 43:377–383.

Nezu Y, Kino Y, Sasagawa N, Nishino I, Ishiura S. 2007. Expression of MBNL and CELF mRNA transcripts in muscles with myotonic dystrophy. Neuromusc Disord 17:306–312.

Onishi H, Kino Y, Morita T, Futai E, Sasagawa N, Ishiura S. 2008. MBNL1 associates with YB-1 in cytoplasmic stress granules. J Neurosci Res 86:1994–2002.

Savkur RS, Philips AV, Cooper TA. 2001. Aberrant regulation of insulin receptor alternative splicing is associated with insulin resistance in myotonic dystrophy. Nat Genet 29:40–47.

SenGupta DJ, Zhang B, Kraemer B, Pochart P, Fields S, Wickens M. 1996. A three-hybrid system to detect RNA–protein interactions in vivo. Proc Natl Acad Sci U S A 93:8496–8501.

Squillace RM, Chenault DM, Wang EH. 2002. Inhibition of muscle differentiation by the novel *muscleblind*-related protein CHCR. Dev Biol 250:218–230.

Takahashi N, Sasagawa N, Suzuki K, Ishiura S. 2000. The CUG-binding protein binds specifically to UG dinucleotide repeats in a yeast three-hybrid system. Biochem Biophys Res Commun 277:518–523.

Takeshita Y, Sasagawa N, Usuki F, Ishiura S. 2003. Decreased expression of alpha-B-crystallin in C2C12 cells that express human DMPK/160CTG repeats. Basic Appl Myol 13:305–308.

Timchenko LT, Miller JW, Timchenko NA, DeVore DR, Datar KV, Lin L, Roberts R, Caskey CT, Swanson MS. 1996. Identification of a (CUG)n triplet repeat RNA-binding protein and its expression in myotonic dystrophy. Nucleic Acids Res 24:4407–4414.

Tsilfidis C, MacKenzie AE, Mettler G, Barcel J, Korneluk RG. 1992. Correlation between CTG trinucleotide repeat length and frequency of severe congenital myotonic dystrophy. Nat Genet 1:192–195.

Vicente M, Monferrer L, Poulos MG, Houseley J, Monckton DG, O'Dell KM, Swanson MS, Artero RD. 2007. Muscleblind isoforms are functionally distinct and regulate alpha-actinin splicing. Differentiation 75:427–440.

Wang LC, Hung WT, Pan H, Chen KY, Wu YC, Liu YF, Hsiao KM. 2008. Growth-dependent effect of *muscleblind* knockdown on *Caenorhabditis elegans*. Biochem Biophys Res Commun 366:705–709.

Warf MB, Berglund JA. 2007. MBNL binds similar RNA structures in the CUG repeats of myotonic dystrophy and its pre-mRNA substrate cardiac troponin T. RNA 13:2238–2251.

Wheeler TM, Krym MC, Thornton CA. 2007. Ribonuclear foci at the neuromuscular junction in myotonic dystrophy type 1. Neuromusc Disord 17:242–247.

Yuan Y, Compton SA, Sobczak K, Stenberg MG, Thornton CA, Griffith JD, Swanson MS. 2007. Muscleblind-like 1 interacts with RNA hairpins in splicing target and pathogenic RNAs. Nucleic Acids Res 35:5474–5486.

Published online 31 August 2009

Nucleic Acids Research, 2009, Vol. 37, No. 19 6477–6490
doi:10.1093/nar/gkp681

MBNL and CELF proteins regulate alternative splicing of the skeletal muscle chloride channel *CLCN1*

Yoshihiro Kino[1,2], Chika Washizu[1], Yoko Oma[2], Hayato Onishi[2], Yuriko Nezu[2], Noboru Sasagawa[2], Nobuyuki Nukina[1] and Shoichi Ishiura[2,*]

[1]Laboratory for Structural Neuropathology, RIKEN Brain Science Institute, 2-1, Hirosawa, Wako-shi, Saitama, 351-0198 and [2]Department of Life Sciences, Graduate School of Arts and Sciences, the University of Tokyo, 3-8-1, Komaba, Meguro-ku, Tokyo, 153-8902, Japan

Received April 8, 2009; Revised July 30, 2009; Accepted August 3, 2009

ABSTRACT

The expression and function of the skeletal muscle chloride channel *CLCN1/ClC-1* is regulated by alternative splicing. Inclusion of the *CLCN1* exon 7A is aberrantly elevated in myotonic dystrophy (DM), a genetic disorder caused by the expansion of a CTG or CCTG repeat. Increased exon 7A inclusion leads to a reduction in *CLCN1* function, which can be causative of myotonia. Two RNA-binding protein families—muscleblind-like (MBNL) and CUG-BP and ETR-3-like factor (CELF) proteins—are thought to mediate the splicing misregulation in DM. Here, we have identified multiple factors that regulate the alternative splicing of a mouse *Clcn1* minigene. The inclusion of exon 7A was repressed by MBNL proteins while promoted by an expanded CUG repeat or CELF4, but not by CUG-BP. Mutation analyses suggested that exon 7A and its flanking region mediate the effect of MBNL1, whereas another distinct region in intron 6 mediates that of CELF4. An exonic splicing enhancer essential for the inclusion of exon 7A was identified at the 5′ end of this exon, which might be inhibited by MBNL1. Collectively, these results provide a mechanistic model for the regulation of *Clcn1* splicing, and reveal novel regulatory properties of MBNL and CELF proteins.

INTRODUCTION

Myotonic dystrophy (dystrophia myotonica, DM) type 1, or DM1, is a genetic disorder with multi-systemic symptoms, such as myotonia, progressive muscle loss, cataracts, cardiac conduction defects, insulin resistance and cognitive impairments (1). DM1 is caused by the expansion of a CTG trinucleotide repeat in the 3′-untranslated region (UTR) of the DM protein kinase (*DMPK*) gene (2–4). Evidence suggests that the expanded CUG repeats transcribed from a mutated allele cause RNA gain-of-function effects that affect the function of other cellular factors. This concept is supported by transgenic mice (HSA^{LR}) expressing an expanded CUG repeat inserted in an unrelated gene (human skeletal actin, *HSA*) that manifest myotonia and abnormal muscle histology (5). Recently, a second locus of DM has been identified, and CCTG repeat expansion in intron 1 of the *ZNF9* gene was found to be causative of DM type 2 (DM2; 6). Remarkably, in the nuclei of cells of patients with both DM1 and DM2, RNA inclusions containing CUG and CCUG repeats, respectively, have been observed (6–8). In addition, abnormalities in RNA metabolism have been found in the cells of DM patients. Splicing of certain genes is misregulated in DM1. These genes include cardiac troponin T (*cTNT/TNNT2*), insulin receptor (*IR*), chloride channel 1 (*CLCN1*), fast skeletal troponin T (*TNNT3*), sarcoplasmic/endoplasmic reticulum Ca^{2+}-ATPase (*SERCA*) 1 and others (9–14). The splicing patterns of some of these genes are also misregulated in DM2 patients and the HSA^{LR} mouse (12,15,16). These results suggest that certain RNA-binding proteins that regulate pre-mRNA splicing of these genes are abnormally influenced by the mutant transcripts containing expanded CUG/CCUG repeats (17).

Two protein families—muscleblind-like (MBNL) and CUG-BP and ETR-3-like factor (CELF) proteins—may play major roles in the pathogenesis of DM. MBNL proteins MBNL1/EXP, MBNL2/MBLL/MLP1 and MBNL3/MBXL/CHCR are orthologs of the *Drosophila* muscleblind protein, which is involved in the terminal differentiation of photoreceptor and muscle cells in the fly (18,19). All three MBNL proteins can colocalize with RNA inclusions of expanded CUG/CCUG repeats in

*To whom correspondence should be addressed. Tel: +81 3 5454 6739; Fax: +81 3 5454 6739; Email: cishiura@mail.ecc.u-tokyo.ac.jp

both DM1 and DM2 cells (20). MBNL1 binds directly to both CUG and CCUG repeat RNA in a length-dependent manner *in vitro* (21,22). Therefore, these proteins are considered to be sequestered by the expanded RNA through direct interactions, and their cellular functions can be disrupted in both types of DM. Remarkably, knockout mice of *Mbnl1* manifest some DM-like symptoms, including myotonia, abnormal muscle histology and cataracts (13). More recently, *Mbnl2* knockout mice were reported to manifest myotonia (23). Importantly, cellular studies have demonstrated that MBNL proteins can directly regulate the alternative splicing of the *cTNT* and *IR* genes, which are misregulated in DM1 patients (24,25). These results strongly support the hypothesis that loss of function of MBNL proteins leads to the misregulation of splicing in DM.

CELF proteins are another protein family involved in the pathogenesis of DM1. CELF proteins CUG-BP/CUGBP1/BRUNOL2, ETR-3/CUGBP2/NAPOR/BRUNOL3, CELF3/TNRC4/BRUNOL1, CELF4/BRUNOL4, CELF5/BRUNOL5 and CELF6/BRUNOL6 are multi-functional proteins that play regulatory roles in translation, RNA editing, mRNA stability, as well as splicing (26–29). CUG-BP regulates the alternative splicing of *cTNT* exon 5, *IR* exon 11 and *CLCN1* intron 2 (9–11). In DM1 patients, the expression of CUG-BP protein is elevated because of protein stabilization induced by PKC-mediated phosphorylation (10,30,31). Moreover, CUG-BP transgenic mice can reproduce some of the muscular abnormalities observed in DM1 or its congenital form, including aberrant splicing and muscle histology (32,33). CUG-BP acts antagonistically against MBNL proteins in the splicing regulation of *cTNT* and *IR* (24,25), suggesting that altered CELF activities, in addition to the loss of MBNL function, can induce aberrant splicing in DM1. However, the extent to which these proteins can account for splicing abnormalities and the pathogenesis of DM remains unclear.

Myotonia is a characteristic symptom of both DM1 and DM2 and has been linked with a loss of function of *CLCN1* chloride channel caused by aberrant splicing of its pre-mRNA in DM patients (11,12). The CLCN1 protein is a muscle-enriched voltage-gated chloride channel and is important for stabilizing the resting potential of muscle membrane (34). More than 50 mutations of *CLCN1* have been found in myotonia congenita, another genetic disorder with myotonia, directly linking defects of *CLCN1* with the pathogenesis of myotonia (35). In DM1 patients, the abnormal inclusion of alternative exons 6B and/or 7A and retention of intron 2 of *CLCN1* have been observed (11,12). These aberrant-splicing patterns can lead to *CLCN1* transcripts containing premature termination codons, resulting in an enhanced degradation of transcripts through the mechanism of nonsense-mediated mRNA decay (NMD), or the production of truncated proteins having a dominant-negative effect (12,36). Consistently, the levels of *CLCN1* mRNA and protein are considerably lower in the muscle of DM patients (11,12). Thus, the misregulated splicing of *CLCN1* in DM1 leads to a reduction in CLCN1 activity, which can be causative of myotonia.

In mouse models expressing an expanded CUG repeat (HSA^{LR}) or lacking *Mbnl1*, the inclusion of exon 7A in mouse *Clcn1* increased, as in human *CLCN1* of DM patients (12,13). It is important to note that the introduction of exogenous MBNL1 into HSA^{LR} mice by viral administration reversed the misregulation of *Clcn1* splicing as well as the myotonic phenotype (37). Furthermore, antisense oligonucleotide (AON)-induced exon 7A skipping resulted in the upregulation of *Clcn1* mRNA and protein levels and eliminated myotonia in both HSA^{LR} and *Mbnl1* knockout mice (38). This suggests that the misregulation of *Clcn1* splicing alone can explain the pathogenesis of myotonia in these mouse models. Therefore, MBNL proteins play an essential role in the splicing regulation of *Clcn1* and are probably involved in the pathogenesis of myotonia in DM. Although the loss of function of MBNL was reproduced in these two mouse models, another pathogenic pathway involving CELF proteins might have been underrepresented in these models, which did not show elevated CUG-BP protein levels (13,16,39). Therefore, it is important to ask whether CELF proteins are involved in the regulation of *CLCN1*/*Clcn1* splicing. Indeed, CUG-BP binds directly to an element in intron 2 and promotes the retention of this intron (11). Furthermore, CUG-BP transgenic mice exhibit increased inclusion of *Clcn1* exon 7A, even though the manifestation of myotonia is not clear (33). Thus, it is important to characterize the roles of MBNL and CELF proteins in the regulation of *Clcn1* splicing to understand the mechanism of myotonia in DM. Although increased exon 7A inclusion is the most frequent abnormality of *CLCN1*/*Clcn1* splicing in DM (12), the mechanism of its regulation is still unclear.

We established a *Clcn1* minigene assay system and identified multiple *cis*- and *trans*-acting factors that regulate the alternative splicing of *Clcn1* exon 7A. The essential role of MBNL proteins in the normal splicing pattern of *Clcn1* was verified. Our results also highlight some CELF proteins as antagonistic regulators against MBNL proteins.

MATERIALS AND METHODS

cDNA clones and constructs

MBNL1 and MBNL2 were amplified by polymerase chain reaction (PCR) from a human skeletal muscle cDNA library (BD Marathon-Ready human cDNA; Clontech). MBNL3 was amplified from a human liver cDNA library. Because the amplified MBNL3 cDNA clones contained an extra exon compared to a previous MBNL3 sequence, this exon was deleted by PCR-mediated mutagenesis. CELF proteins ETR-3, CELF3, CELF4, CELF5 and CELF6 were amplified from cDNA libraries of either brain or skeletal muscle of human origin. CUG-BP was amplified from pSRD/CUG-BP (40). Forward primers for the amplification of these cDNAs contained BamHI, BglII, or EcoRI sites, whereas the reverse primers contained either SalI or XhoI sites to add these restriction sites to

the PCR products. Fragments of these cDNAs were inserted into the BamHI-XhoI or EcoRI-XhoI site of pSecDK, a mammalian expression vector with a myc-tag that was modified from pSecTagA (Invitrogen) to delete the Igκ chain leader sequence. Constructs encoding GST-MBNL1$_{40}$ has been described previously (22). The *Clcn1* minigene fragment covering exons 6 to 7 was amplified from mouse genomic DNA by PCR using the primer pair Clcn1-Fw and Clcn1-Rv, into which a restriction site for BamHI or SalI was added. Similarly, the corresponding fragment of human *CLCN1* was amplified using primers CLCN1-Fw and CLCN1-Rv. The minigene fragments were ligated into pGEM-T Easy vector (Promega). The minigene fragments in pGEM-T Easy were cleaved by BamHI and SalI and then subcloned into the BglII-SalI site of pEGFP-C1 (Clontech). A series of deletion mutants of *Clcn1* was generated by PCR-mediated mutagenesis. To construct heterologous minigenes, we inserted alternative exons with flanking regions such as *Clcn1* 451–720 into the BglII-SalI sites of pEGFP-Tpm2-ex1-2 vector (see Supplementary 'Materials and Methods' section). Primer sequences are listed in Supplementary Table S1. Detailed information on the sequences and construction of mutant minigenes is available upon request. DM18 and DM480 contain a fragment of the 3′ region of DMPK with a CTG18 and interrupted CTG480 repeats, respectively (Supplementary Figure S4).

R-miR, a vector modified from pcDNATM6.2-GW/EmGFP-miR (Invitrogen), was utilized for RNA interference (RNAi) experiments. R-miR contains a cDNA fragment of monomeric RFP (mRFP) in place of EmGFP and an Esp3I recognition site introduced downstream of mRFP. DNA fragments corresponding to a portion of an artificial microRNA (Supplementary Table S2) were designed using BLOCK-iT RNA Designer (Invitrogen website) and inserted into the Esp3I site of R-miR.

The FANTOM3 clone plasmids encoding murine Mbnl3 (E430034C16), Cugbp1 (4432412L08), Cugbp2/Etr-3 (9530098D08) and Celf4 (C130060B05) used for testing RNAi efficiency in Neuro2a cells were provided by Dr Hayashizaki (41). Murine Mbnl1 and Mbnl2 were amplified from a mouse brain cDNA library. The N-terminal regions of Mbnl1, Mbnl2 and Mbnl3 and the full-length open reading frames of Cugbp1, Cugbp2 and Celf4 were amplified with primers containing restriction sites, digested by the restriction enzymes, and inserted into the BglII-SalI site of the pEGFP-C1 vector. All constructs were confirmed by sequencing.

Cellular splicing assay

Cells transfected with plasmids for the expression of a protein and a minigene were harvested 48 h post-transfection. Typically, cells were cultured in 12-well plates and transfected with 0.5 μg plasmids for protein expression (or cognate empty vector) and 0.01 μg plasmids for the expression of a minigene. Total RNA was extracted and purified using either the acidic guanidine phenol chloroform method or RNeasy Mini kit (Qiagen) including DNase treatment. Typically, 1.0 μg total RNA was reverse-transcribed using the ThermoScript RT-PCR System (Invitrogen) or Revertra Ace -α- (TOYOBO) with a 1 : 1 mixture of oligo dT and random hexamer as primers. Minigene fragments were amplified by PCR using a fluorescein isothiocyanate (FITC)-labeled forward primer for the 3′ region of the EGFP sequence (FITC-GFP-Fw) and a gene-specific reverse primer (Clcn1-Rv for *Clcn1* or CLCN1-Rv for *CLCN1* Supplementary Table S1). For *Tpm2*-based minigenes, primers FITC-GFP-Fw and Tpm2-ex2-splicing-Rv2 were used for amplification. PCR products were resolved by 2.0–2.5% agarose gel electrophoresis. By sampling at multiple cycles, the cycle numbers of PCR were adjusted such that the amplification was within the logarithmic phase. The fluorescence of PCR products was captured and visualized by LAS1000 or LAS3000 (FUJIFILM). The intensity of band signals was quantified using Multigauge software (FUJIFILM). The ratio of exon 7A inclusion in *Clcn1* and *CLCN1* was calculated as (7A inclusion)/(7A inclusion + 7A skipping) × 100.

Quantitative PCR

Gene-specific primers were designed using Primer Express software (Applied BioSystems) and are listed in Supplementary Table S3. These primer sets were mixed with cDNA samples and Power SYBR Green PCR Master Mix (Applied BioSystems). Real-time amplification and quantification were performed using an ABI7700 (Applied BioSystems) following the manufacturer's protocol.

Gel shift analysis

GST and GST-MBNL1 were purified as described previously (22). Oligo DNA templates corresponding to Clcn1(473–518) (CTGCCCAGGCACGGTCTGCAACA GAGAAGCACGACGGGCGAGGCAGCCCTATAGT GAGTCGTATTACCCC), Clcn1(GAA) (CTGTTCTTC TTCTTCCTGCAACAGAGAAGCACGACGGGCGA GGCAGCCCTATAGTGAGTCGTATTACCCC), and Clcn1(a504c) (CTGCCCAGGCACGGGCTGCAACAG AGAAGCACGACGGGCGAGGCAGCCCTATAGTG AGTCGTATTACCCC) were purchased from Invitrogen and annealed with another DNA fragment for the T7 promoter (GGGGTAATACGACTCACTATAGGG). Using this partial duplex as a template, we transcribed RNA using T7 RNA polymerase (MEGAscript T7 kit; Ambion). The RNA was purified by phenol–chloroform extraction followed by ethanol precipitation. The purified RNA was treated with alkaline phosphatase, then labeled by T4 polynucleotide kinase in the presence of γ-^{32}P-ATP. The labeled RNA was purified using a Nucaway spin column (Ambion). The procedures and reaction mixture used in the gel shift analysis are described in our previous report (22).

Ribonucleoprotein immunoprecipitation

Ribonucleoprotein immunoprecipitation (RIP) was performed as described previously (42), with minor modifications. The amount of co-precipitated minigene